

**Effects of Ultrafine Particulate Matter Exposure in an Animal Model of Neurodegenerative
Disease**

Final Report

Agreement No. 14-315

Principal Investigator: Arthur K. Cho, Ph.D.
Department of Environmental Health Sciences
Fielding School of Public Health
University of California, Los Angeles
Los Angeles, CA 90095-1792

Prepared for:
State of California Air Resources Board
Research Division
P.O. Box 2815
Sacramento CA 95812

January 29, 2019

Disclaimer

The statements and conclusions in this Report are those of the contractor and not necessarily those of the California Air Resources Board. The mention of commercial products, their source, or their use in connection with material reported herein is not to be construed as actual or implied endorsement of such products.

Acknowledgements

This project was funded under the ARB's Dr. William F. Friedman Health Research Program. During Dr. Friedman's tenure on the Board, he played a major role in guiding ARB's health research program. His commitment to the citizens of California was evident through his personal and professional interest in the Board's health research, especially in studies related to children's health. The Board is sincerely grateful for all of Dr. Friedman's personal and professional contributions to the State of California. We wish to also acknowledge the interest and support of the California Air Resources Board in this project, in particular Dr. Lori Miyasato who, in addition, guided the Principal Investigator through the administrative aspects of the project.

The research was a joint effort of the Environmental Health Sciences and the Department of Molecular and Medical Pharmacology at the University of California Los Angeles (UCLA: Arthur Cho, William Melega, Debra Schmitz), with the Air Pollution Health Effects Laboratory at the Department of Medicine, University of California, Irvine (UCI: Michael Kleinman). We acknowledge the able assistance of the following members of the Air Pollution Health Effects Laboratory; Andrew J. Keebaugh and David A. Herman who collected and processed the air samples, Amanda Ting and Samantha Renusch who participated in the animal procedures, and Melanie S. Goldberg of the Blurton-Jones Laboratory who was responsible for breeding the transgenic mice, confirming their genetic status by PCR, and provided detailed information regarding husbandry of the h α -Syn transgenic animals.

This Report was submitted in fulfillment of ARB Agreement No. 14-315, "Effects of Ultrafine Particulate Matter Exposure in an Animal Model of Neurodegenerative Disease" under the sponsorship of the California Air Resources Board. Work was completed as of October 2018.

Executive Summary

This project was designed to test the hypothesis that air pollution (AP) components from a Southern California site could induce the development of Parkinson's Disease (PD)-like behavioral and brain pathology in an animal model. The exposures were performed at the Air Pollution Health Effects Laboratory at UC Irvine. This location is proximate to the heavily trafficked I405 and CA73. As such, this locale provided a unique opportunity to assess the effects of AP in a context not associated with extreme AP conditions, e.g., Mexico City or Beijing, but nonetheless one that may impact the health and well-being of individuals living in Irvine, CA, and in other areas with similar magnitudes of AP exposure.

The hypothesis was based on the premise that reactive chemical species in AP mixtures are responsible for adverse health effects by interacting with cellular targets to elicit responses such as inflammation. We chose as an animal model a strain of transgenic mice expressing human alpha-synuclein (α -Syn), a protein marker that accumulates in PD. These mice develop behavioral deficits and neuropathology in the course of their development that parallel aspects of the human disease. Additionally, wild-type littermates of the same mouse strain were included in the study design in order to provide insights into the effects of the AP exposure without a α -Syn contribution.

The mice were exposed to concentrated UFPM of $<0.18 \mu$ (CAPS) generated by the Versatile Aerosol Concentration Enrichment System (VACES) or filtered air from which volatile organic compounds (VOCs) had been removed at the UC Irvine Laboratory of Dr. Michael Kleinman. After a 22 week exposure period, the mice were subjected to behavior tests and then sacrificed for brain analyses of AP-associated neurochemical alterations. In parallel, $PM_{2.5}$ and VOCs of the ambient air were collected with a Tisch sampler and subjected to chemical and cellular assays to obtain a quantitative description of their chemical and cellular properties to aid in the interpretation of the biological results.

Results

The research was divided into four tasks, exposure (task 1), in vivo responses (task 2), brain pathology measurements (task 3), and chemical and biological characterization of the exposure atmosphere (task 4).

Task 1. The exposure atmosphere at UC Irvine was found to be lower in mass (90 vs. 114 to 213 $\mu\text{g}/\text{m}^3$), elemental carbon (8 vs. 5 to 42 $\mu\text{g}/\text{m}^3$) but most notably organic carbon (15 vs. 54 to 159 $\mu\text{g}/\text{m}^3$) than that found in earlier studies of VACES exposed animals in other Los Angeles Basin sites, but the exposure period was considerably longer at 22 weeks compared to 6 weeks for the longest previous study.

Task 2. Three motor tests (vertical pole descent, challenging beam traversal, nestlet shredding/nest building) and a cognitive test (Y maze alternations) were performed on each animal prior to and following the exposure period. For the h α -Syn mice, the AP exposure did not effect changes that could be attributable uniquely to h α -Syn overexpression. Yet, in the challenging beam test, both the h α -Syn mice and wildtype mice showed significant deficits in hind limbs slips while traversing the beam. That type of deficit is considered a behavioral marker for the detection of early onset motor disorders in animal models of neurodegeneration. Deficits in the other motor and cognitive tests were not observed. Changes in those tests appear to be contingent on decreases in the integrity of dopamine and norepinephrine brain systems. Such decreases were not detected in this study following AP exposure.

Task 3. The hippocampus and striatum from each animal was removed following the exposure period and analyzed for relevant markers of neurotoxicity, i.e., tumor necrosis factor alpha (TNF α), interleukin 6 (IL6), hemeoxygenase-1 (HO-1) and the relevant neurotransmitters, norepinephrine (NE) and dopamine (DA). Levels of human alpha-Synuclein (h α -Syn) were also measured to assess progress of PD-like brain pathology in the transgenic animals. Prior to actual analysis of the brain samples, recovery experiments TNF α and IL6 were performed on control mouse brain to assess assay sensitivity. The results indicated that TNF α levels were too low in the brain samples to be significant whereas IL6 levels were only marginally higher. In an effort to enhance the IL6 sensitivity, we subjected a pooled homogenate of hippocampus to Centricon based concentration and analysis. Those results showed a trend toward higher levels upon AP exposure for both wild type (WT) and transgenic (h α -Syn) animals but the differences were not significant. As a confirmation of the minimal effects of the exposure, significant changes were not measured DA and NE neurotransmitter levels following exposure.

In the study design, we had chosen the AP exposure to occur during the h α -Syn mouse development time interval of ~ 4 to 9 months of age when PD-like brain and behavior deficits begin to manifest in this mouse strain. Our hypothesis was that the AP exposure would accelerate the onset of those deficits and result in larger magnitudes of brain and behavioral deficits which could be detected by our assays. However, although trends toward higher levels of hippocampus h α -Syn and IL6 were observed, the differences were not significant. Thus, minimal changes for the behavioral and neurochemical brain pathology parameters in striatum and hippocampus were associated with exposure to VACES-CAPS.

Task 4. PM2.5 and VOCs of the ambient air prior to VACES concentration were subjected to in vitro-based chemical analyses to obtain quantitative data for assessment of chemical reactivity (prooxidants and electrophiles), and for biological analyses (inflammation/ TNF α and adaptation/HO-1) of the VOC samples by assays in a mouse macrophage cell line. In general, the prooxidant and electrophile contents of the Irvine samples were lower than those found for

other sites in the Los Angeles Basin (e.g., communities near railyards) as part of a SCAQMD funded study and consistent with these lower chemical properties, the cell responses were also somewhat lower. Correlation analyses of the chemical properties and biological responses showed the Irvine VOC samples to exhibit minimal correlation between their chemical properties and cell responses. Instead, the prooxidant content of the corresponding PM_{2.5} was a better predictor of the cell response intensities. The organic carbon contents of the Irvine samples were found to positively correlate with their pro-inflammatory potency and negatively correlate with anti-inflammatory response, also differing from the other VOC whose chemical reactivity positively correlated with anti-inflammatory responses. In summary, the results of this analysis indicated the ambient Irvine VOC differed both quantitatively and qualitatively from the other LA Basin VOC in the Los Angeles Basin thus limiting the scope of the interpretations regarding the minimal effects of the exposure.

Conclusions

The protocol used in this study was designed to assess the effects of exposure to concentrated ultrafine particles (<0.18 μ m) from ambient air in Irvine, CA on behavioral and neurochemical markers associated with Parkinson's disease-like development in wild type and transgenic (α -Syn) mice that express the human PD marker, alpha synuclein. The results generally did not show significant changes reflective of development of PD-like behavioral and brain pathology.

This conclusion should be tempered however, with the caveats revealed in the parallel studies examining the properties of the exposure atmosphere that have been compared with those from Mexico City, where neurotoxic markers associated with PD development were found and other communities in the Los Angeles Basin. The CAPS exposure was lower in total mass per m³, organic and elemental carbon, prooxidant content of the particles, and lower chemical reactivities in the VOC fraction. Although the exposure period of 22 weeks was considerably longer than that used in prior studies using VACES concentrated particles, the cumulative effect of exposure to low level toxins may not have affected the target organs because of their ability to reduce chemical challenges with enzymatic detoxification procedures.

The results did demonstrate the value of monitoring the chemical properties of air pollution mixtures and performing in vitro analyses to characterize AP mixtures, for they allow design of predictive studies with useful parameters.

Although exposure of the mice to CAPS did not affect PD-like development, there are qualifying concerns that limit the scope of the conclusions. They are:

1. The ambient air at Irvine differed from other Los Angeles Basin locations (tested by us) that may have been better locations for the study. Further, the VACES-based concentration may not have provided an exposure atmosphere with sufficient quantities

of relevant reactive components to elicit changes in cellular responses that could be measured.

2. We did not characterize the VACES generated atmosphere to which the animals were exposed so its properties may not be reflected as a 12 fold increase of the ambient particles.
3. The VACES atmosphere does not contain the ambient VOC whose physical properties provide them ready access to the brain and their concentration by 12 fold could have had significant effects.

Future studies

1. A more comprehensive set of analytical protocols are needed, e.g., chemical and cellular analyses of the VACES generated CAPS atmosphere for a more relevant description.
2. The San Bernardino area of the LA Basin may be a better site for such a study, based on its chemical and cellular properties,

Contents

1. Introduction	10
1.1 Air pollution	10
1.1.1 Perspective of air pollutants	10
1.2 Parkinson's disease	15
1.2.1 Background.....	15
1.2.2. Alpha-Synuclein - a marker of PD pathology in humans and its expression in transgenic mice as an animal model of PD.....	15
2.0 Study tasks	16
2.1 Task 1. AP exposure conditions	16
2.1.1 Background and procedures of AP collections.....	16
2.1.2 Results	23
2.2 Task 2: In Vivo Responses - Motor and cognitive behavior assessments	24
2.2.1 Motor responses.....	25
2.2.2 Cognitive Responses.....	29
2.3 Task 3: Brain pathology assessments	30
2.3.1 Background.....	30
2.3.2 Results	31
2.4 Task 4: Chemical and biological characterization of PM	37
2.4.1 Background.....	38
2.4.2 Results	43
2.5 Summary and general discussion	52
2.5.1 Review of the in vivo and in vitro aspects of the project.	52
3.0 References	57
Appendix 1: Abbreviations	63
Appendix 2: Animal cohorts and calendar	66
Appendix 2 - Legend for Animal cohorts and calendar	67
Appendix 3: Selection and characteristics of the animal model	67
Appendix 4: Statistical analysis parameters for the hα-Syn mice studies	69

List of figures

Figure 1.1.1	Reactive components of air pollution.....	11
Figure 1.1.2	Reactions of active species found in air pollution.....	13
Figure 1.1.3	Lipid peroxidation.....	14
Figure 1.1.4	Reactions of atmospheric reactive species with protein nucleophiles.....	15
Figure 2.1.1	VACES schematic.....	17
Figure 2.1.2	Reactions of the DTT assay.....	18
Figure 2.1.3	The dihydroxybenzoic acid (DHBA) assay.....	19
Figure 2.1.4	Reactions in the glyceraldehyde-3-phosphate dehydrogenase (GAPDH) assay.	21
Figure 2.1.5	Prooxidant content of ambient PM_{2.5}.....	24
Figure 2.2.1	Pole Test.....	25
Figure 2.2.2	Beam traversal challenge.....	27
Figure 2.2.3	Nestlet shredding test.....	28
Figure 2.2.4	Y maze spontaneous alternations.....	30
Figure 2.3.1	Recovery of TNFα from mouse brain homogenates.....	32
Figure 2.3.2.	IL-6 levels in hippocampus.....	33
Figure 2.3.3	HO-1 levels in hippocampus.....	34
Figure 2.3.4	Striatum dopamine content.....	35
Figure 2.3.5	Hippocampus norepinephrine content.....	36
Figure 2.3.6	hα-Syn Content in Striatum and Hippocampus.....	36
Figure 2.3.7	Summary of Hippocampus hα-Syn and IL-6 Content.....	36
Figure 2.4.1	Air pollutants and their cellular targets.....	40
Figure 2.4.2	Reactive components of ambient air in Irvine (UCI) and other sites in the Los Angeles Basin.....	44
Figure 2.4.3.	Expression levels of HO-1 and TNFα following stimulation by vapor phase components from Irvine collections.....	46
Figure 2.4.4	Organic carbon (OC) content vs. cell responses; Irvine samples.....	48
Figure 2.4.5	Cell responses to vapor phase components plotted against correlated prooxidant assays.....	51

List of tables

Table 1.1.1	Examples of reactive species found in air pollutant mixtures.....	12
Table 2.1.1.	DTT activity of quinones in ambient air samples.....	19
Table 2.1.2.	Prooxidants and their DHBA activity.....	20
Table 2.1.3	Average EC and OC exposures for all cohorts (Mean $\mu\text{g}/\text{m}^3 \pm \text{SE}$).....	23
Table 2.1.4	CAPS properties of prior VACES studies.....	23
Table 2.3.1	Neurochemical measurements of brain samples.....	31
Table 2.4.1.	Comparison of PM prooxidant properties.....	44
Table 2.4.2	Summary of chemical and biological properties of ambient Irvine PM_{2.5} and vapors.....	46
Table 2.4.3	Pearson analysis of chemical and cellular data from Irvine.....	46

Table 2.4.4 Summary of chemical and biological properties of SCAQMD Railyard PM_{2.5} and vapors.....	49
Table 2.4.4A. Comparison of the vapor phase properties from Irvine and other Los Angeles Basin sites at 3 m³.	49
Table 2.4.5 Pearson correlation analysis of SCAQMD Railyard PM_{2.5} and vapors	50
Table 2.4.6 Comparison of Pearson correlation results from Irvine and SCAQMD Railyard sites	51
Table 2.5.1 Comparison of <i>in vivo</i> and <i>in vitro</i> studies	52

1. Introduction

The CARB project was designed to test the hypothesis that mice overexpressing human alpha-synuclein (α -Syn) and wild type mice that are exposed to PM_{2.5} (CAPS) concentrated from ambient air will develop behavioral and brain deficits analogous to those observed in Parkinson's Disease (PD). We recognized that the ambient air in Irvine, the site of our exposure chambers was likely to be much less harmful compared to that in Mexico City (Calderon-Garciduenas, Solt et al. 2008), the location of a major study of children that identified early brain changes. Accordingly, we used the Versatile Aerosol Concentration Enrichment System (VACES) in an established exposure protocol (Araujo, Barajas et al. 2008, Campbell, Araujo et al. 2008, Kleinman, Araujo et al. 2008) to closely approximate the Mexico City atmosphere. The exposure itself was a more natural one, i.e., normal inhalation in exposure chambers rather than direct injection of concentrated air samples. In order to provide which we hoped would be a sensitive PD animal model we used transgenic mice expressing α -Syn, a marker protein of PD brain pathology. As these animals mature, they express behavior and neurochemical changes that have been associated with aspects of PD, and by exposing them to the CAPS at a time of their growth associated with these changes, we felt they would provide a sensitive model for testing our hypothesis. The study also included quantitative analyses of the Irvine exposure atmosphere in terms that reflected our perspective of the nature of air pollutants; those data were used to provide a comparative analysis of ambient air reactivities between Irvine and Mexico City. Our perspective is summarized below.

1.1 Air pollution

1.1.1 Perspective of air pollutants

Although the ambient atmosphere contains a multitude of compounds, our research focus has been on those reactive species likely to participate in immediate reactions with targets in cells and physiological fluids. These species are presented to the organism in two physical states, particles of varying sizes and volatile species, as shown in Figure 1.1.1.

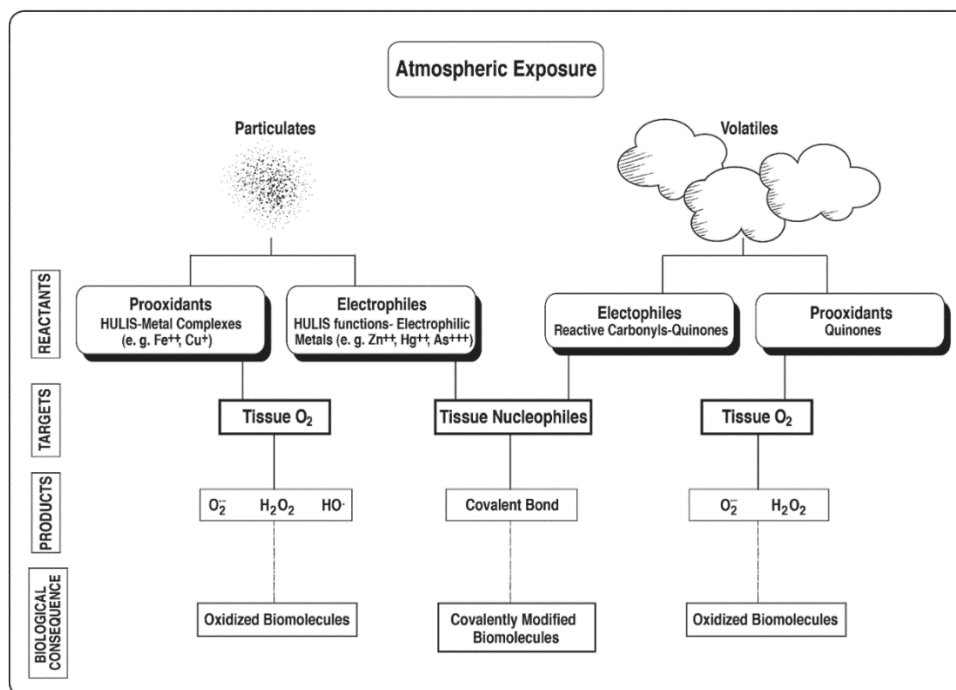


Figure 1.1.1 Reactive components of air pollution.

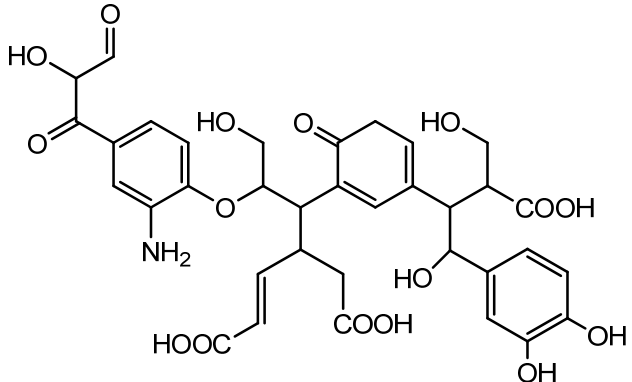
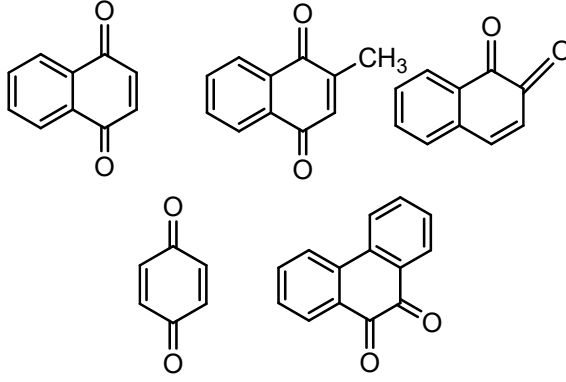
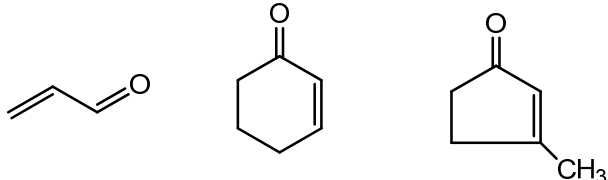
Two types of reactive chemical species, electrophiles and prooxidants are present in the atmosphere in the particulate and vapor phases. Electrophiles form covalent bonds with tissue nucleophiles and covalently modify them. Prooxidants generate the reactive oxygen species, superoxide (O_2^-), hydrogen peroxide (H_2O_2) and hydroxyl radical ($OH\bullet$). These reactive species can be particulate or volatile and exert their actions with targets determined by their physical and chemical properties, initiating two generalized responses, oxidative or electrophilic stress, to which much of the adverse health effects of air pollutants have been attributed.

We define prooxidants as chemical species that catalyze the transfer of electrons from biological substrates such as NADPH and ascorbate to oxygen, generating one or more of the reactive oxygen species, superoxide (O_2^-), hydrogen peroxide (H_2O_2) and hydroxyl radical ($OH\bullet$). The second class of reactants are electrophiles; this species form covalent bonds with reactive centers on receptive biomolecules called nucleophiles. Acrolein is an example of an organic electrophile; it forms covalent bonds with nucleophilic centers on protein such as the thiolate of a cysteine residue. Inorganic electrophiles include arsenic and zinc.

Examples of these species identified in the atmosphere are shown in Table 1.1.1. Organic prooxidants include polymeric polyhydroxy aromatics found in humic-like substances (HULIS) of air pollutants (Ghio, Stonehuerner et al. 1996), transition metals and quinones (Cho, Di Stefano et al. 2004, Valavanidis, Fiotakis et al. 2006, Jakober, Riddle et al. 2007). HULIS can also complex transition metals such as iron and copper and the resulting complex can be sufficiently lipid-soluble to be extractable with polar organic solvents (Shinyashiki, Eiguren-

Fernandez et al. 2009). Lower molecular weight volatile organic electrophiles, e.g., acrolein, have also been identified in the vapor phase. The metals arsenic and zinc are inorganic electrophiles. It should also be pointed out that ozone also reacts with organic compounds in the atmosphere to generate electrophilic species (Yang, Ma et al. 2018).

Table 1.1.1 Examples of reactive species found in air pollutant mixtures

Chemical class	Structures	Properties
Humic-like substances (HULIS)		Electrophiles and prooxidants (Ghio, Stonehuerner et al. 1996, Davies, Ghabbour et al. 2001, Lin and Yu 2011, Zheng, He et al. 2013, Verma, Fang et al. 2015)
Redox-active Metals	Fe, Cu, Cr, Ni	Prooxidants (Valko, Morris et al. 2005)
Electrophilic Metals	Hg, Pb, V, As	Electrophiles (LoPachin and Barber 2006) (Wu, Bromberg et al. 2013) (Shinkai, Sumi et al. 2006)
Quinones		Electrophiles and prooxidants (Kumagai, Shinkai et al. 2012) (Cho, Di Stefano et al. 2004, Valavanidis, Fiotakis et al. 2006, Jakober, Riddle et al. 2007, Delgado-Saborit, Alam et al. 2013)
Reactive carbonyls		Electrophiles (Jakober, Charles et al. 2006)

Toxicologically relevant reactions by components of atmosphere - reactions of prooxidants and electrophiles.

Stage 1: Interactions with initial targets

The toxicologically relevant species of AP includes prooxidants, substances capable of catalyzing the reduction of oxygen to reactive oxygen species and electrophiles. These reactivities are shown in Figure 1.1.2 below; with 1,2-naphthoquinone (1,2-NQ) and iron (Fe^{II}) as examples of prooxidants (reactions (1) to (3)) and acrolein as an electrophile (reaction (4)). These species interact initially with their biological targets which are typically a reducing species such as ascorbate, NADH, or thioredoxin to initiate reaction (2) for the formation of hydrogen peroxide or a tissue nucleophile such as thiolate. Reactions (1) and (2) show the catalytic nature of prooxidant action as the prooxidant cycles using NADH as the reducing agent. A similar cyclic reaction can occur with Fe^{II} with ascorbate as the reducing agent. Reaction (4) shows covalent bond formation between the electrophile, acrolein, and a thiolate function on a macromolecule.

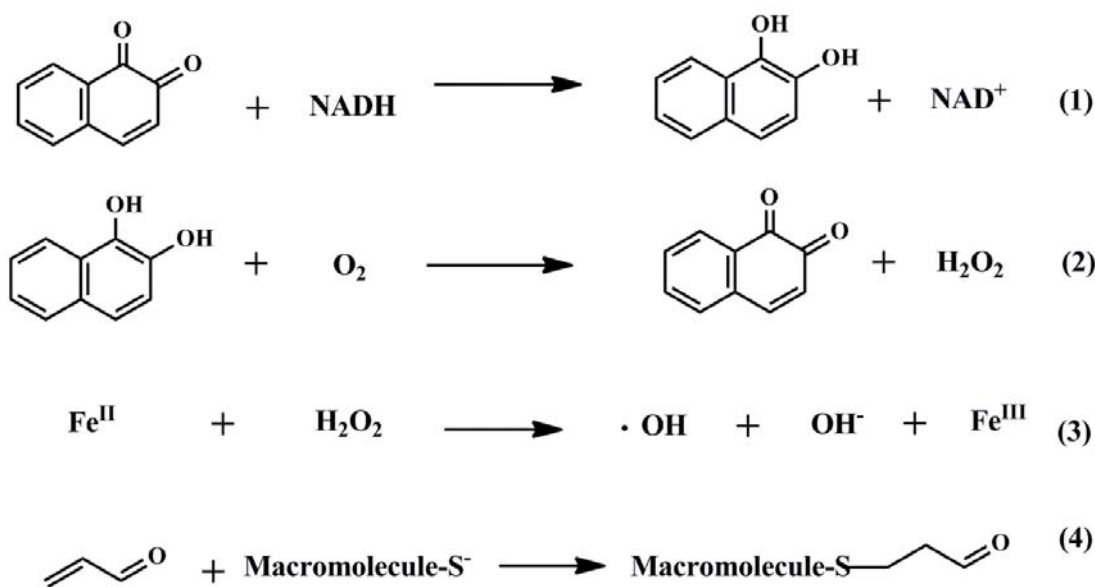
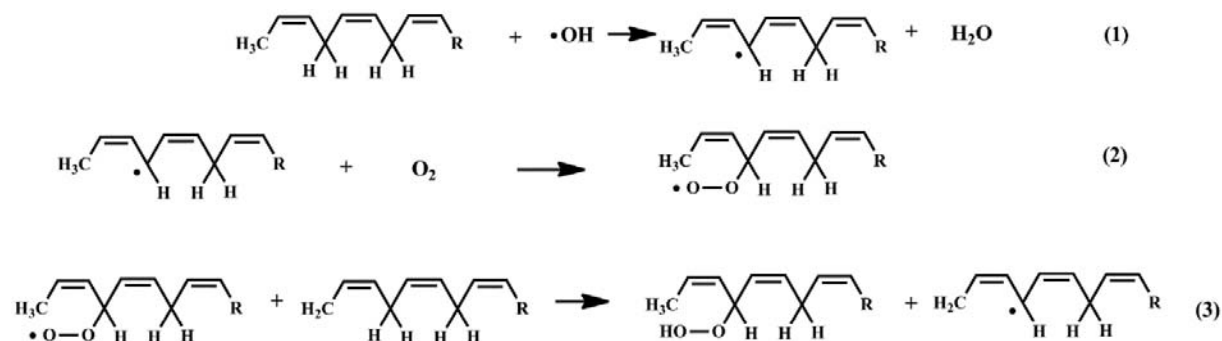


Figure 1.1.2 Reactions of active species found in air pollution

The reactions of 1,2-naphthoquinone (1,2-NQ) (reactions 1 and 2); ferrous ion (reaction 3) and acrolein (reaction 4) are shown as examples of compounds that have been found in air pollution mixtures. Reactions (1) and (2) demonstrate the 1,2-NQ catalyzed reduction of oxygen to hydrogen peroxide nicotinamide adenine dinucleotide (NADH). In the reaction 1,2-NQ is acting as a prooxidant; it is catalyzing the electron transfer reaction between NADH and oxygen. Reaction (3) is the reduction of hydrogen peroxide to the highly reactive hydroxyl radical by ferrous ion, the so-called Fenton reaction. Reaction (4) shows the modification of a macromolecule by addition of acrolein to the thiolate function on the macromolecule, an example of the Michael addition reaction that results in the modification of the target macromolecule.

Stage 2: Initiation of the biological response

Figure 1.1.3 show reactions associated with the initiation of the biological response. Thus, reactions (1) through (3) of Figure 1.1.3 summarize the lipid peroxidation reaction sequence caused initially by hydroxyl radical, generated in Stage 1. Hydroxyl radical is the most reactive of the reactive oxygen species that includes superoxide and hydrogen peroxide and can abstract hydrogen atom from available sites at diffusion rates.

**Figure 1.1.3 Lipid peroxidation.**

The highly reactive hydroxyl radical, generated by a prooxidant, hydrogen peroxide and an electron source, abstracts a hydrogen atom from the labile hydrogens of the polyunsaturated terminal of a fatty acid (1). The resulting radical then adds oxygen to form a peroxy fatty acid (2) which can also abstract a hydrogen atom to form the peroxy lipid and another radical (3). Reaction (3) is a chain reaction, so called because of the continuous formation of the radical lipid.

Figure 1.1.4 shows additional reactions. Thus, hydrogen peroxide is less reactive but capable of oxidative reactions as shown in reaction (4) forming sulfenic acids with thiolate anion. This reaction is a common pathway in cell signaling reactions in which hydrogen peroxide is the signaling molecule (see for example, (Poole and Nelson 2008)). Figure 1.1.4 shows reactions of a tissue nucleophile shown as a thiolate, with (1) hydrogen peroxide to form the corresponding sulfenic acid and with an electrophile shown as acrolein to form a covalent bond in reaction (2). These are the reactions that can induce cellular oxidative stress and trigger a series of signaling pathways that lead to inflammation and exacerbate existing pathologies.

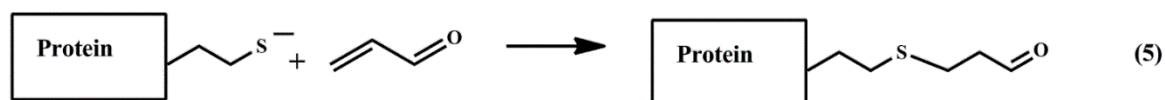
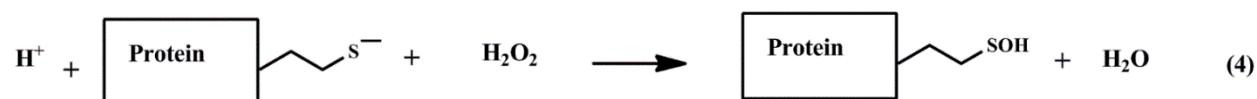


Figure 1.1.4 Reactions of atmospheric reactive species with protein nucleophiles

Two reactions are shown: Reaction (4) is the oxidation of a protein thiolate, the ionized form of a thiol, by hydrogen peroxide to form a sulfenic acid. Reaction (5) is the addition reaction between the thiolate and the electrophilic acrolein, to form a covalently modified protein. Sulfenic acids can be reduced by cellular reactions whereas the modified protein cannot, and requires resynthesis to replace the lost protein.

Summary

The perspective of the exposure atmosphere of this project focuses on the actions of reactive chemical species in the atmosphere that react with relevant chemical species in the biological system to initiate cellular responses that ultimately result in the observed tissue response. To describe this atmosphere in quantitative terms we performed the chemical analyses summarized in Section 2.1.

1.2 Parkinson's disease

1.2.1 Background

A growing body of epidemiological and clinical evidence suggests that environment-associated oxidative stress may be involved in the development and progression of Parkinson's disease (PD) (Finkelstein and Jerrett 2007, Calderon-Garciduenas, Solt et al. 2008, Migliore and Coppede 2009, Genc, Zadeoglulari et al. 2012). Of particular significance is a recent report on the contributions of air pollution (AP) to neurodegenerative diseases in children exposed to AP in the Mexico City area. These children showed an early brain imbalance in genes involved in oxidative stress (Calderon-Garciduenas, Franco-Lira et al. 2013) accompanied by a misfolding of proteins in those brain areas associated with early stages of both Alzheimer's and Parkinson's disease. Based on these findings, the authors suggested that oxidative stress resulting from exposure to air pollutants in early life could lead to the development of neurodegenerative diseases in later life. Further evidence for a potential AP contribution to neurodegenerative diseases has been obtained from experimental studies in rats in which exposure to diesel exhaust particles (DEP) and vapors over a wide concentration range (35-991 particles/m³) effected neurochemical changes in the nigrostriatal dopamine system consistent with oxidative stress-based inflammation (Levesque, Surace et al. 2011).

1.2.2. Alpha-Synuclein - a marker of PD pathology in humans and its expression in transgenic mice as an animal model of PD

The development of PD is marked by the increase in fibrils of alpha-synuclein (α -Syn) histologically demonstrated in Lewy bodies (Eschbach and Danzer 2013) in brain regions. α -Syn is a relatively small, soluble protein of ~ 14 kDa and is abundantly expressed in the nervous system, comprising 1% of total cytosolic protein. In presynaptic terminals, α -Syn is present in close proximity to, but not within synaptic vesicles (Stefanis 2012). Its function remains not well

understood but its aggregation into oligomers is thought to be the first step in the developing pathology, possibly by disrupting synaptic vesicles, altering lipid membranes, and promoting calcium efflux (Ono 2017). Thus, oligomers of α -Syn are thought to be neurotoxins, but there remain many unknowns. For example, some recent studies have shown that it is the increases in the soluble α -Syn that are associated with Alzheimer's and PD pathology (Stefanis 2012; Larson et al. 2012; Dettmer, Selkoe et al. 2016). Nonetheless, identification of this association between α -Syn and PD has led to the development of corresponding animal models for PD studies. Transgenic animals overexpressing human α -Syn protein (h α -Syn) have now been shown to progressively exhibit behavioral and neurochemical changes throughout the lifetime of the animal that mimic aspects of PD [see for example, (Amschl et al. 2013, Chesselet et al. 2012)]. Thus, this transgenic animal model is currently regarded as a viable animal PD model, particularly in contradistinction to acute chemical toxin-associated animal models. Accordingly, to assess the effects of AP on the development of PD-like pathophysiology, we used a D-line transgenic mice (Amschl et al. 2013) which overexpress h α -Syn and also exhibit some behavioral changes analogous to those observed in PD. The animals were kindly made available to us by Dr. Matthew Blurton-Jones of the Department of Biology at UCI and were transported from Blurton-Jones Lab to the UCI Kleinman Lab for the duration of the study. The h α -Syn mice, aged ~4 months of age at the start of the study, were exposed to concentrated AP within exposure chambers for 5h/d for 4d/wk for 22 wks (Kleinman et al. 2008).

2.0 Study tasks

2.1 Task 1. AP exposure conditions

To expose transgenic overexpressing h α -Syn and wild type mice to PM_{2.5} and to filtered air devoid of VOCs for a 22 week exposure period.

2.1.1 Background and procedures of AP collections

VACES concentrators

The VACES concentrates ambient PM_{2.5} with an impactor, the output of which is connected to a warm hydration chamber that hydrates the particles to increase their size and mass (Kim, Jaques et al. 2001, Kim, Jaques et al. 2001). From this chamber the hydrated and concentrated PM_{2.5} are cooled and then passed into a heated drying chamber to remove the water. The dried particles are then introduced into the exposure chamber (see figure 2.1.1). The VACES is capable of including PM_{2.5} by factors up to 30 fold but in this project was set to concentrate by 10 fold.

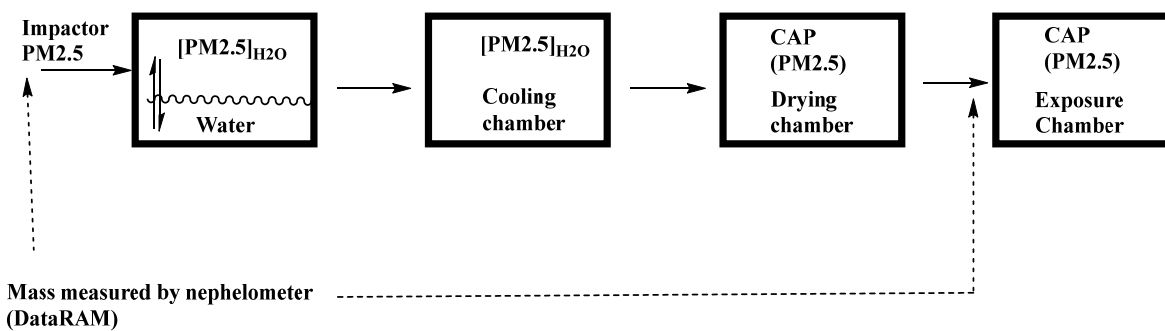


Figure 2.1.1 VACES schematic

Quantitative analysis of chemical reactivities

Prooxidant analyses. Quantitative analyses of the reactive species in the atmosphere are critical for an assessment of potential toxicity resulting from exposure to AP mixtures. Accordingly, we and others have developed assay procedures that provide quantitative data on AP prooxidants. Our laboratory has developed two prooxidant assays: 1) a dithiothreitol (DTT) based oxygen reduction assay for total prooxidants, and 2) a Fenton reaction-based assay that measures generation of hydroxyl radical by transition metal catalysis of salicylic acid conversion to dihydroxybenzoic acid (DHBA). DTT is a dithiol, whose adjacent thiol groups makes it highly effective in electron transfer or reduction reactions similarly to the cellular reducing agent, thioredoxin (Kumagai, Koide et al. 2002). As shown in Figure 2.1.2, DTT reduces the prooxidant by one electron as shown in reactions (1) and (2), and the reduced prooxidant reduces oxygen to superoxide in reaction (3) followed by disproportionation of the superoxide to oxygen and hydrogen peroxide (reaction (4)). The net reaction, reaction (5), is the prooxidant catalyzed formation of hydrogen peroxide with the oxidation of reduced DTT. In the assay DTT is consumed with a rate proportional to the concentration and potency of prooxidants. Since DTT can also be oxidized by metal ions such as iron and copper (Netto and Stadtman 1996, Kachur, Held et al. 1997), the contribution of metals to the total DTT-based redox activity can be determined by adding the metal chelator, diethylenetriamine pentaacetate (DTPA, 20 μM), (Di Stefano, Eiguren-Fernandez et al. 2009)) to a separate set of samples and subtracting that result from the total DTT consumed. The units used are the nanomoles of DTT consumed per minute per m^3 or mass of air sample.

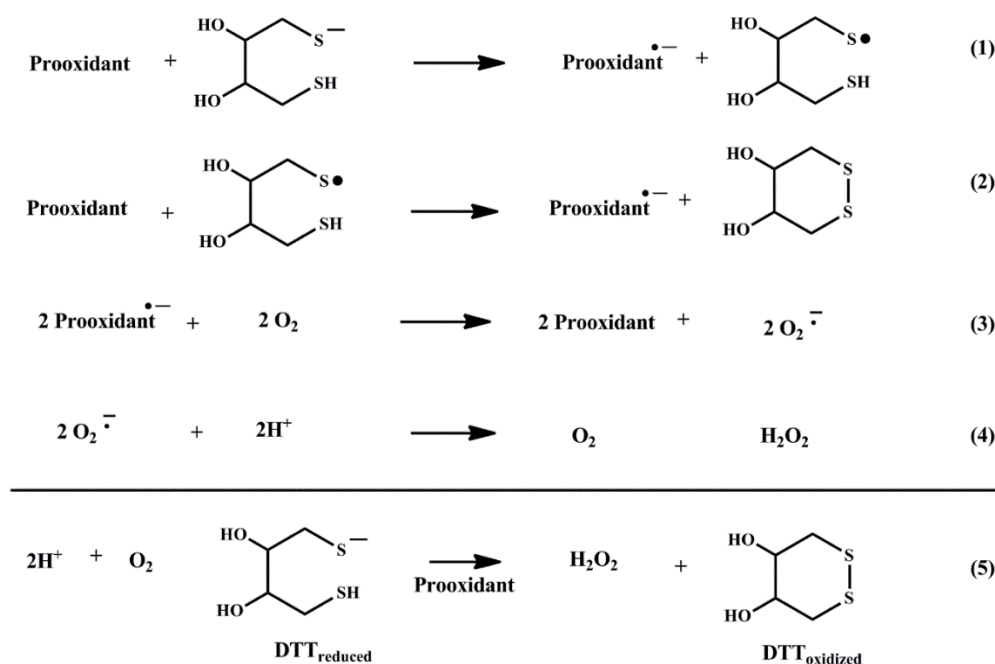


Figure 2.1.2 Reactions of the DTT assay

Prooxidants present in the AP sample, are reduced by one electron (reactions (1) and (2)), the reduced prooxidant then reduces oxygen to superoxide (3), which disproportionates to hydrogen peroxide and oxygen (4). The net reaction (5) is the prooxidant catalyzed reduction of oxygen by DTT, whose consumption is measured in the assay (Cho, Sioutas et al. 2005)

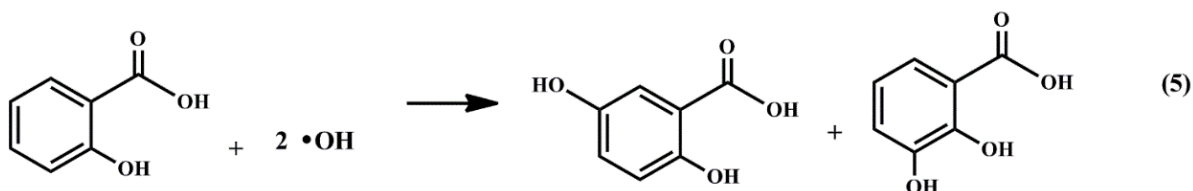
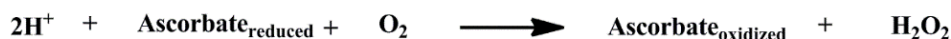
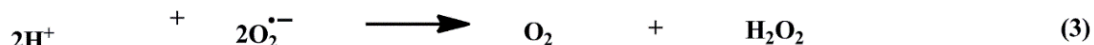
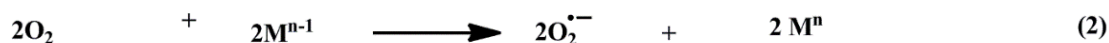
The DTT reaction and quinones

In previous studies, we assessed the hypothesis that atmospheric quinones contribute to the prooxidant activity of air pollutants by developing a quantitative assay for four quinones found in the diesel exhaust and ambient air (Cho, Di Stefano et al. 2004). We applied the DTT assay to a study of vapor phase samples from three California communities (Alpine, Santa Maria and Lake Elsinore) in which the content of four quinones was determined as part of a collaborative study with the Environmental Health Department at USC. Using these concentrations and the DTT based prooxidant activities of each quinone, we assessed their contribution to the total DTT activities. Table 2.1.1 shows the results of this analysis with the percent of prooxidant content attributable to the measured quinones in the samples. Note that only about 10% of the observed DTT activity was accounted for by the measured quinones, suggesting other quinones or redox-active species are present in the mixture. This apparently low recovery of reactivity in terms of the four measured quinones likely reflects the presence of other quinones as subsequent quinone assays have measured high concentrations of up to 15 quinones in air samples collected at trafficked roadsides (Valavanidis, Fiotakis et al. 2006, Delgado-Saborit, Alam et al. 2013, Totlandsdal, Ovrevik et al. 2014).

Table 2.1.1. DTT activity of quinones in ambient air samples

	Obsvd DTT activity	Conc of 1,4-NQ	Conc of 1,2-NQ	Conc of 9,10-PQ	Total Calcd DTT activity*	% of observed
Location	nmol DTT/min*m ³	ng/m ³	ng/m ³	ng/m ³	nmol DTT/min*m ³	100* Calcd/Obsvd
Alpine	0.08	0.15	0.88	0	0.01	10.76
Santa Maria	0.11	0.19	0.75	0	0.01	8.56
Lake Elsinore	0.09	0.28	1.23	0.01	0.01	15.99

*Calculated DTT activity from $\sum(\text{concentration of quinone ng/m}^3) * (\text{DTT activity/ng})$

**Figure 2.1.3 The dihydroxybenzoic acid (DHBA) assay**

The prooxidant in this assay is shown as a metal (M^n) of charge “n”. The metal in the n state is reduced by ascorbate by one electron to the n-1 state (1), which then reduces oxygen to superoxide (2). The superoxide disproportionates to oxygen and hydrogen peroxide. Hydrogen peroxide is reduced by the metal in the n-1 state in the Fenton reaction, generating hydroxyl radical (3). The formation of both hydrogen peroxide and hydroxyl radical are thus dependent

on the availability of a reducing species such as ascorbate to reduce the metal ion. In the assay, the formed hydroxyl radical reacts rapidly with salicylate to form the dihydroxybenzoic acids shown in (5), which are quantitated by HPLC and electrochemical detection (Di Stefano, Eiguren-Fernandez et al. 2009).

Reactions of prooxidants in the DHBA assay

Table 2.1.2 compares the behavior of different prooxidants (20 μ M) in this assay, in which both ascorbate consumption and DHBA formation were measured. Note that the quinones do not generate DHBA but do consume ascorbate. As mentioned above, they react with ascorbate and oxygen to form superoxide and hydrogen peroxide but only the metals catalyze the formation of DHBA by hydroxyl radical (Fenton reaction). Consistent with metal involvement, the reaction is blocked by DTPA. Table 2.1.2 also shows copper is a better catalyst than iron in the reaction.

Table 2.1.2. Prooxidants and their DHBA activity.

Prooxidant	Ascorbate consumption nmoles/min*nmol	DHBA formation nmoles/min*nmol
1,4-NQ	1.98	0
9,10-PQ	3.05	0
Fe ^{II}	0.55	0.01
Cu ^{II}	1.72	0.02

Electrophiles and electrophilic reactions

Electrophilic reactions result in covalent bond formation between the two reactive species, nucleophiles and electrophiles. In the context of toxicology, the nucleophile is typically a cellular macromolecule or intermediate and the toxic species or exogenous reactor is an electrophile. Both inorganic and organic species can be electrophilic. For example, zinc and mercury ions as well as vanadates readily react with cellular nucleophilic centers such as those with cysteine thiolate functions (Samet and Tal 2010, Wu, Bromberg et al. 2013) as do reactive carbonyls and quinones (Kumagai, Shinkai et al. 2012).

The GAPDH assay

To determine electrophile content in an AP sample, we established an assay using glyceraldehyde-3-phosphate dehydrogenase (GAPDH) as a nucleophile (Shinyashiki, Rodriguez et al. 2008) in reactions summarized in figure 2.1.4 with acrolein as the electrophile. The enzyme catalyzes the oxidation of glyceraldehyde 3-phosphate (GAP) to 1,4-diphosphoglycerate in a reaction involving the formation of a covalent bond between the carbonyl carbon of GAP and a thiolate on the enzyme. This thiolate appears to have minimal selectivity and

forms covalent bonds with multiple electrophiles (see comments in (Rodriguez, Fukuto et al. 2005)) and for that reason provides a useful target for electrophiles. The cellular relevance of this assay is in the reactive thiolate which we use as the nucleophile in reaction (4) of Figure 1.1.4 with acrolein as the electrophile. Reactive thiolates are found in toxicologically relevant proteins such as protein tyrosine phosphatase 1B (Samet, Silbajoris et al. 1999, Bayram, Ito et al. 2006, Iwamoto, Sumi et al. 2007) and the transcription factor, Nuclear factor (erythroid-derived 2)-like 2 (Nrf2) (Dinkova-Kostova, Holtzclaw et al. 2002), as well as GAPDH (Iwamoto, Nishiyama et al. 2010). The assay measures the extent of irreversible inactivation of the enzyme caused by covalent bond formation between the catalytic thiolate and electrophiles.

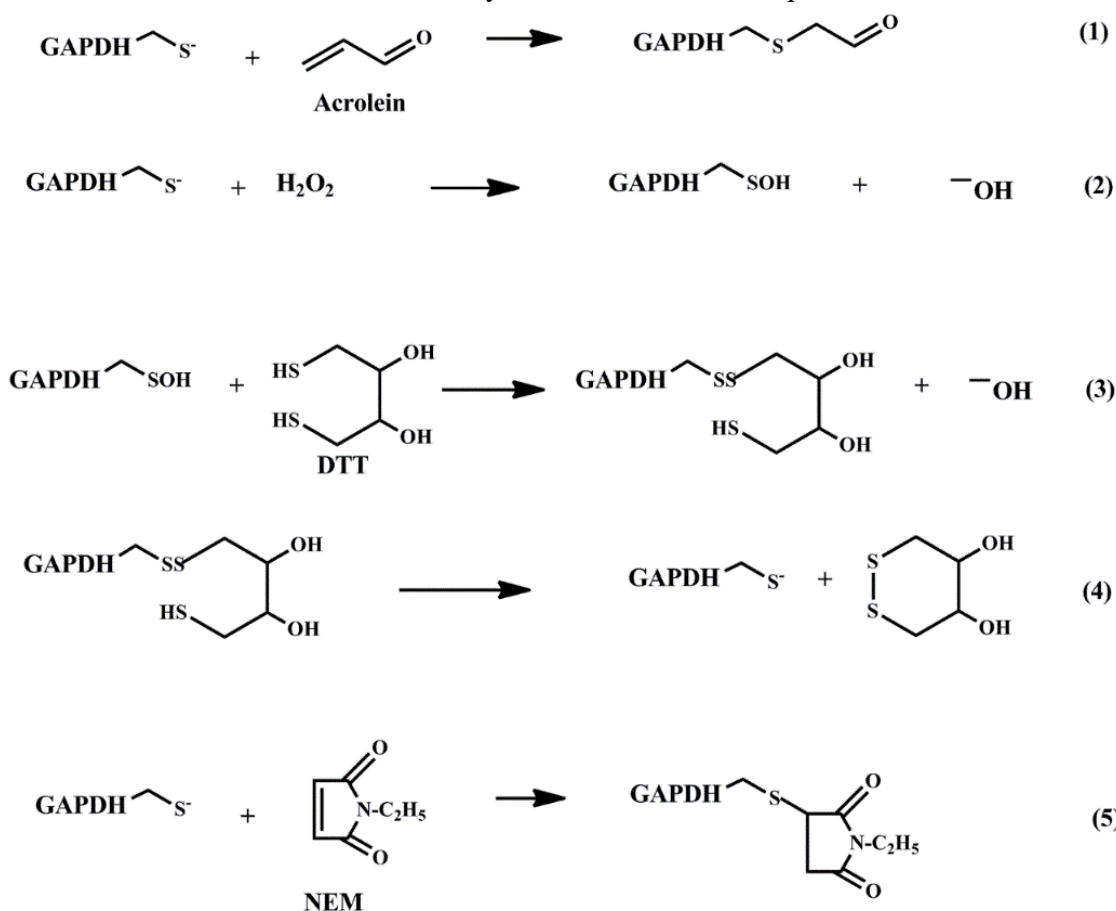


Figure 2.1.4 Reactions in the glyceraldehyde-3-phosphate dehydrogenase (GAPDH) assay. Electrophiles react with the thiolate groups on the enzyme according to reactions (1) or (2). Only reaction (1) is the irreversible inactivation of enzyme. Reaction of the thiolate with hydrogen peroxide, (2), converts the thiol to sulfenic acid which is reversed with DTT according to (reactions (3) and (4)). The residual enzyme activity is determined and inactivation normalized to the standard electrophile N-ethyl maleimide (NEM), (5). To insure measurement of this event, the assay is performed in the absence of oxygen and the product(s) of the reaction

are treated with DTT to reduce oxidized thiol (Shinyashiki, Rodriguez et al. 2008) generated by H₂O₂ in reactions (2) and (3), leaving only covalently modified enzyme.

Application of the GAPDH assay

In previous studies of ambient vapor samples collected from Riverside, CA, we have identified the formation of AP-derived adducts to multiple nucleophiles that include GAPDH, protein tyrosine phosphatase 1B, a regulatory enzyme in the activity of the epidermal growth factor receptor and Kelch-like ECH-associated protein 1 (KEAP 1), the regulatory protein for Nrf2 (Iwamoto, Nishiyama et al. 2010). Matrix-assisted laser desorption ionization time-of-flight mass spectrometry (MALDI TOF/MS) was used to identify apparent molecular weight changes in specific proteins as a result of covalent modification. These studies provided unequivocal evidence for covalent modification of specific proteins by atmospheric electrophiles. The procedure also provided an averaged molecular weight of 90-200 daltons for the adducted species, indicating they were of low molecular weight. Other investigators have demonstrated analogous molecular weight changes in hemoglobin and albumin in humans following exposure to reactive electrophiles (Carlsson and Tornqvist 2016, Carlsson, Aasa et al. 2017) using MALDI MS procedures. This general phenomenon of electrophile addition to biological substrates is now referred to as “adductomics” (Rappaport, Li et al. 2012, Carlsson, von Stedingk et al. 2014).

Exposure procedure

Ambient air for the exposures was drawn into the VACES at a flow rate of 300 liters per min (via a 2- m long and 7.5-cm diameter aluminum duct that minimized particle losses due to electrostatic deposition. The inlet to the duct was about 2.2 m above the ground. The concentrated aerosols were delivered to whole-body animal exposure chambers. Each exposure chamber was a sealed unit, sectioned for housing 18 mice per chamber. Temperature and airflow were controlled during the exposures to ensure adequate ventilation, minimize buildup of animal-generated contaminants (dander, ammonia and CO₂) and to avoid thermal stresses.

Animal exposure conditions

Wild type and hα-Syn transgenic mice, age 4 months at the start of the study, were grouped into 4 cohorts; each cohort contained 4 subgroups (hα-Syn +/-AP exposure and wild type +/-AP exposure). Exposures began on July 7, 2015 and continued until January 18, 2016. Each cohort was exposed for 5h/d for 4d/wk for 22 wks (~ 5 mo); See Appendix 2. Grouping into multiple cohorts and staggering of the initiation of each cohort exposure by 2 – 3 wks allowed for animals to be age-matched both within and across cohorts. There remained significant overlap across all 4 exposure periods, indicating that all exposed mice were exposed to essentially the same AP content. There were practical time limitations in the number of animals that could be processed for behavioral assessment and brain acquisition at the end of each exposure period (we considered it relevant to obtain the behavioral assessments and conduct the sacrifice procedures within similar time windows ~ 4 -6 h to avoid potential diurnal effects on outcome measures).

2.1.2 Results

CAPS samples from the current study

Table 2.1.3 summarizes organic (OC) and elemental (EC) carbon of ambient and VACES based based atmosphere (CAPS) to which the four cohorts of animals were exposed.

Table 2.1.3 Average EC and OC exposures for all cohorts (Mean $\mu\text{g}/\text{m}^3 \pm \text{SE}$)

		Cohort 1	Cohort 2	Cohort 3	Cohort 4
Air	OC	0.94 \pm 0.28	0.84 \pm 0.28	1.22 \pm 0.39	2.30 \pm 0.76
	EC	0.85 \pm 0.2	0.51 \pm 0.2	0.42 \pm 0.18	0.32 \pm 0.16
CAPS	OC	14.53 \pm 2.65	15.27 \pm 2.56	16.42 \pm 1.32	15.36 \pm 1.87
	EC	7.65 \pm 1.36	8.18 \pm 1.30	8.58 \pm 1.32	7.89 \pm 1.20

Table 2.1.4 CAPS properties of prior VACES studies

Study	Exposure UFP ¹ concentration Conc ($\mu\text{g}/\text{m}^3$).	EC	OC ($\mu\text{g}/\text{m}^3$)	Comment
(Campbell, Oldham et al. 2005)	282.5	5.73 %	47.80 %	Mice, 2 week exposure: Site: Downtown Los Angeles Found: NFkB and IL1 increased in brain
(Kleinman, Sioutas et al. 2007)	213 \pm 95	42 \pm 37 ($\mu\text{g}/\text{m}^3$)	159 \pm 27 ($\mu\text{g}/\text{m}^3$)	Mice, 2 week exposure Site: Adjacent to freeway Lung effects determined..
(Kleinman, Araujo et al. 2008)	114	8.9 ($\mu\text{g}/\text{m}^3$)	54 ($\mu\text{g}/\text{m}^3$)	Mice 6 week exposure; Site: Downtown Los Angeles AP1, NFkB increased in brain
Current	90 \pm 10	8.1 ($\mu\text{g}/\text{m}^3$)	15.4 ($\mu\text{g}/\text{m}^3$)	Mice: 22 week exposure Site: UC Irvine campus.

Table 2.1.3 compares the general properties of the CAPS with those from the earlier studies which had resulted in changes in brain markers for inflammation. In the CAPS for the current study were lower than those in other sites but with a longer exposure period. The most notable difference was in the organic carbon content, which was about 1/3rd that of the other studies.

The CAPS concentration of 90 $\mu\text{g}/\text{m}^3$ is in the low range of the exposures used by Levesque et al., who exposed rats to diesel exhaust particles at concentrations between 35 and 991 $\mu\text{g}/\text{m}^3$ (Levesque, Surace et al. 2011) over 6 months. By comparison our exposure paradigm was shorter and used CAPS concentrated ambient PM_{2.5} rather than diesel exhaust particles.

The chemical properties of the ambient air processed by the VACES were determined in PM_{2.5} samples and the corresponding VOCs collected simultaneously with Tisch samplers following our published protocol (Eiguren-Fernandez 2015). The PM_{2.5} samples were subjected to the DTT prooxidant analysis with and without DTPA to determine total (without DTPA) and organic (with DTPA) prooxidant content. Results from those studies are summarized below (Figure 2.1.6). There was a higher DTPA insensitive prooxidant content (inverted triangles) than we had found in other Los Angeles Basin sites (Eiguren-Fernandez (2015) during the initial 10 weeks of the exposure.

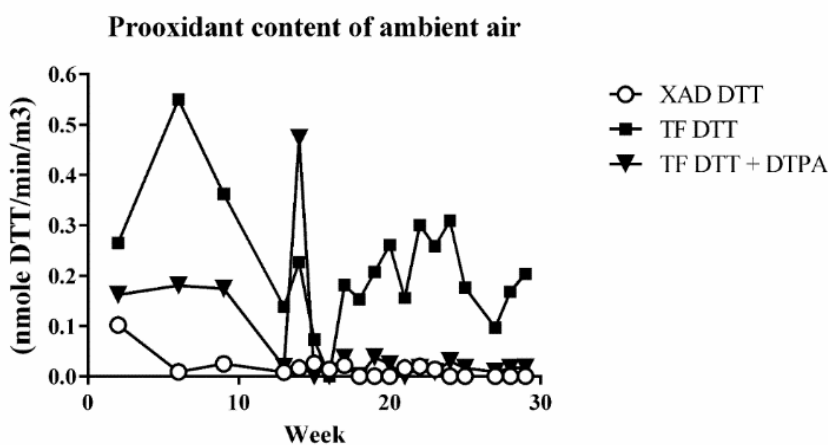


Figure 2.1.5 Prooxidant content of ambient PM_{2.5}.

Results of DTT based prooxidant assays performed on Teflon coated filters TF (PM_{2.5}) and XAD extracts (VOCs) from ambient air samples collected with a Tisch sampler in parallel with the VACES. Assay results following diethylenetriamine pentaacetate (DTPA) are used to determine levels of non-metal prooxidants.

2.2 Task 2: In Vivo Responses - Motor and cognitive behavior assessments

All animals were evaluated for motor and cognitive behavior responses, 4d after their final week of 22 wks of consecutive exposure. A series of 4 behavioral tests were used to evaluate development of PD-like behaviors in the hα-Syn transgenic and wild type mice. The tests used had been validated in previous studies on this strain of hα-Syn transgenic mice and their wild type littermates (Amschl et. al.2013) or in studies with animal models of PD. Accordingly, there was comparison data in published literature that extended across the same age range as our studies. The domains covered by these tests assessed behavioral pathologies that parallel aspects of PD (e.g., basal ganglia integrity, locomotor activity, gait, fine motor skills, cognitive function, spatial memory). For example, the beam test detected decreases in locomotor speed (time required to traverse beam) as well as fine motor control (number of missteps as the beam width narrows throughout its length).

2.2.1 Motor responses

Pole test – Background and Methods

This test was used to assess aspects of basal ganglia function that have been associated with movement disorders in PD (Matsuura et al. 1997). Briefly, the base of a vertical wooden pole was placed in a cage filled with bedding material. Animals were then placed head-up on top of the pole. When the mice were placed on top of the pole, head-up, they oriented themselves downward and descended the length of the pole back into the cage. After two days of training, animals received five test trials. Time to orient downward (t-turn) and total time to descend (t-total) represented the measures of motor coordination. The data are reported as mean \pm SEM.

In previous studies, deficits in pole test performance were observed in mice that had either significant decreases ($> 60\%$) in striatum dopamine content that were toxin-induced, or by increases in striatum α -Syn content. We suggest that in our study the absence of such motor deficits was primarily related to the absence of significant AP-associated striatum dopamine deficits. Also, in previous studies of α -Syn transgenic mice using other promoters of its expression, higher expression levels of α -Syn in striatum relative to hippocampus resulted in motor deficits. We did not observe significant increases of α -Syn in either the hippocampus or the striatum following AP exposure.

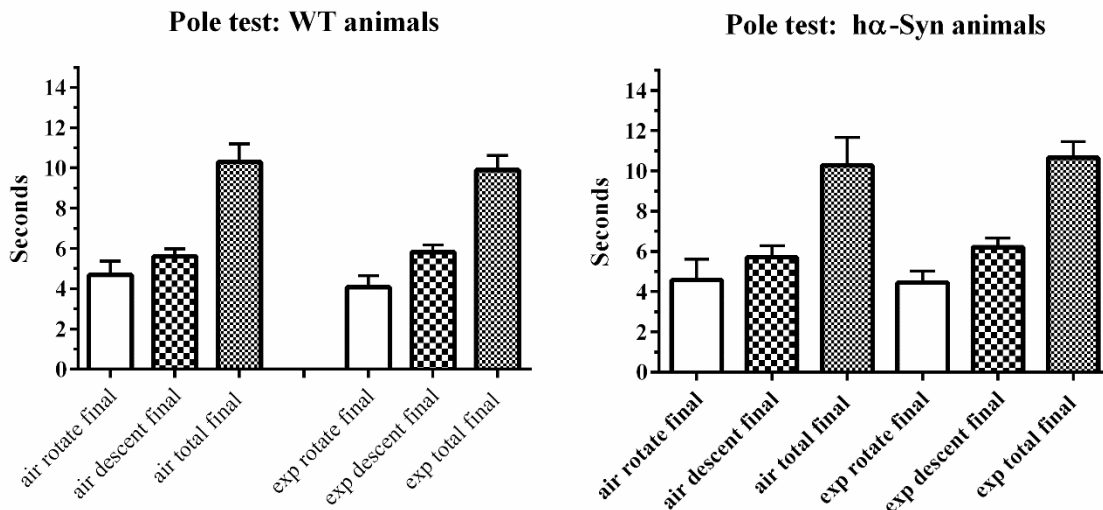


Figure 2.2.1 Pole Test.

The pole test was conducted 4 days after the completion of 22 weeks of AP or air exposure (final). Time (sec) to orient downward (rotate final) and total time to descend (descent final),

and the sum of the two times (total final). Data are expressed as mean \pm SEM for 5 trials for each measure for N = 16-19 per group. Significant differences were not observed for either criterion for the wild type and h α -Syn transgenic mice (Student's t-test; $p > .05$). See Appendix 4 for statistical parameters.

Pole test – Results and discussion

The final responses in the pole test are shown in figure 2.2.1. No significant differences were observed in air and exposed animals from either strains. In previous studies, deficits in pole test performance were observed in mice that had either significant decreases ($> 60\%$) in striatum dopamine content that were toxin-induced, or by increases in striatum h α -Syn content. We suggest that in our study the absence of such motor deficits was primarily related to the absence of significant AP-associated striatum dopamine deficits as determined from the post-mortem brain analysis. Also, in previous studies of h α -Syn transgenic mice using other promoters of its expression, higher expression levels of h α -Syn in striatum relative to hippocampus resulted in motor deficits. We did not observe significant increases of h α -Syn in either the hippocampus or the striatum.

2. Beam traversal challenge test – Background and methods

This test was used to assess fine motor coordination and balance, and considered sensitive to varying degrees of nigrostriatal dopaminergic dysfunction in genetic mouse models (Fleming et al. 2004). In brief, a plexiglass beam 1 m length total, and comprising of four (25 cm length) sections that gradually decreased in diameter from 3.5 cm to 0.5 cm in 1 cm increments was used. Animals were trained to traverse the beam (from widest to narrowest) directly into the animal's home cage. Each mouse received two days of training (5 trials each) followed by testing on the third day. During the testing phase, a wire mesh grid (1 cm²) of corresponding beam width was placed over the beam and subjects were video-recorded while traversing the beam, over 5 trials. The total time taken to traverse the beam, and number of foot slips off the beam were determined over the 5 trials and averaged. Grid faults /steps, steps, and time to traverse were used for analysis. The results expressed as 'final – initial' were analyzed by paired t-tests; the mean values for each condition are shown in Figure 2.2.2.

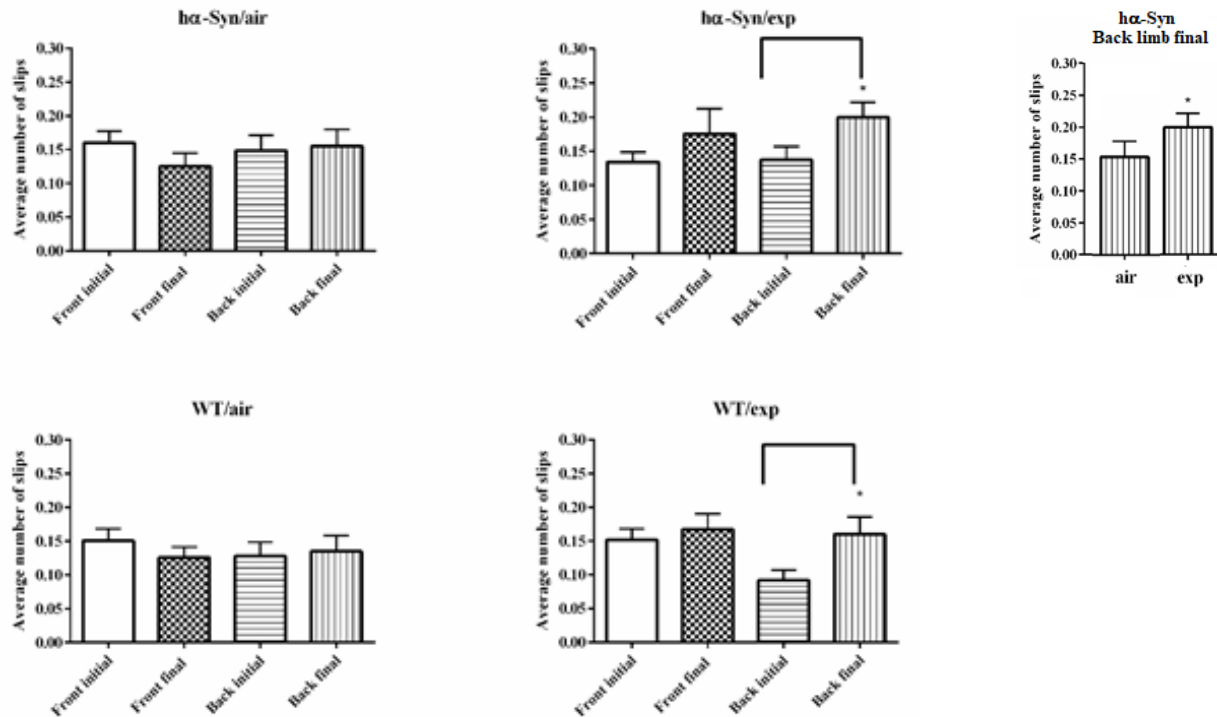


Figure 2.2.2 Beam traversal challenge.

The beam traversal test was conducted at 1 week prior to the start of the exposure (initial) and at 4 days after the completion of 22 weeks of AP or air exposure (final). The numbers of foot slips for front and back limbs of mice as the mice traversed the beam were separately analyzed.

Results shown are means \pm SEM for $N = 16-19$ per cohort. * $p < .05$.

See Appendix 4 for statistical parameters.

Beam traversal challenge – Results and Discussion

A two-way ANOVA with repeated measures for hα-Syn/exp vs WT/exp did not show a significant interaction $F(1,32)$, $p = .188$. Paired Student's t-tests were then used to analyze pre- and post-exposure effects in hα-Syn and WT groups; significant increases in back limb foot slips were observed for both groups post-exposure (final); hα-Syn/exp, $p = .0345$; WT/exp, $p = .0385$. Back limb slips (final) for hα-Syn/exp (0.1994 ± 0.02 , mean, SE) were significantly increased relative to hα-Syn/air (0.1371 ± 0.019); Student's t-test, $p = .0425$.

We were unable to attribute these differences to an associated brain measure that was obtained in

these animals, post-mortem. A possible explanation is that subtle alterations in dopamine function may not be reflected by corresponding changes in striatal dopamine levels, and yet differences in functional dopamine system activity may underlie the observed motor impairments on the challenging beam traversal test.

3. Nestlet Shredding Test – Background and methods

This test was used to assess fine motor skills for a species-typical behavior; impairments are associated with hippocampal damage (Deacon and Rawlins 2006). To test the nest building behavior, mice were housed individually in cages containing wood chip bedding and one 5×5 cm² of pressed cotton ('nestlet'). No other nesting material was present. Manipulation of the nestlet and the constitution of the built nest was photographed at 2 and 18 h for later assessment by analysts blinded to the conditions. Assessment of the quality of the nestlet was based on a predefined five-point nest-rating Likert scale between 1 and 5 in 0.5 increments (1- untouched nestlet → 2 – 4 - graded result → 5 – well-shaped nest using all nestlet material). The results were assessed as group differences at 2h and 18 for each condition, with statistical analysis by Mann–Whitney U-test (Deacon, 2012). The results are shown in Figure 2.2.3

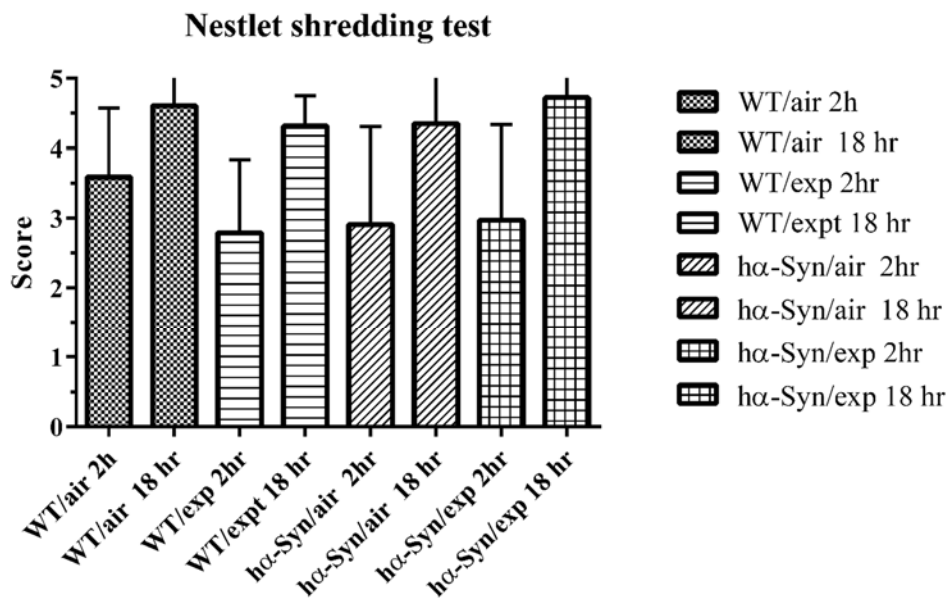


Figure 2.2.3 Nestlet shredding test.

Results are shown for each condition at 2 and 18 h after mice were presented with nestlet material (mean ± SEM; N = 16-20 animals per condition). All groups of animals showed advancement in their nestlet building as a function of time. Significant differences in nestlet

building were not observed between wild type and h α -Syn groups at either the 2 or 18h time points as assessed by Mann–Whitney U-test ($p > .05$). See Appendix 4 for statistical parameters.

Nestlet shredding test – Results and Discussion

Nesting behavior has been reported to be impaired by brain lesions including those to the hippocampus and medial prefrontal cortex (Deacon, 2006). In this study, all groups showed improvements in their nest building between the 2 and 18 h time points which may be attributable to absence of significant alterations detected in the hippocampus for NE, and the inflammatory markers IL-6 and TNF α (see figures 2.3.5 and 2.3.7) following AP exposure. The 2 h timepoint was considered an adequate early timepoint for detecting potential differences in initial delays of nestlet building following AP exposure. For example, the 1 – 5 scores of all h α -Syn mice at the 2 h timepoint remained relatively low: ~ 35% scored between 1 - 2.5; 50% scored between 3 - 4; and only 15% scored between 4.5 - 5. Thus, the test was sensitive to the detection of potential differences in low scores if they had occurred. The 18 h timepoint provided a later measure of nestlet building in which a lower than ‘5’ score may have suggested a different type of contributing brain deficit than that for the 2 h timepoint.

2.2.2 Cognitive Responses

Y-Maze Spontaneous Alternation Test – Background and methods

This test was used to assess spatial memory as a quick and simple measure of retention that avoids the need for extensive training and the use of conventional reinforcers. In compromised animals, it is thought to provide a measure of short-term spatial memory capacities through interactions with or modulation of central cholinergic processes, chiefly in the hippocampus and associated structures (Hughes, 2004; Deacon and Rawlins, 2006).

Testing occurred in a Y-shaped maze with three plastic arms at a 120° angle from each other. After introduction to the center of the maze, the animal was allowed to freely explore the three arms, where it should show a tendency to enter a less recently visited arm. Alternations were defined as “a consecutive entry in three different arms” over a 7 min period while an overhead video camera tracked their behavior (Magen et al. 2012) for later analysis. Both the percentage of alternations as a fraction of total visits, and the total number (#) of arm visits, (i.e., total entries into any of the three arms during the 7 min) were calculated and expressed for each cohort (n = 16 - 20) as mean \pm SEM. The results are shown in Figure 2.2.4,

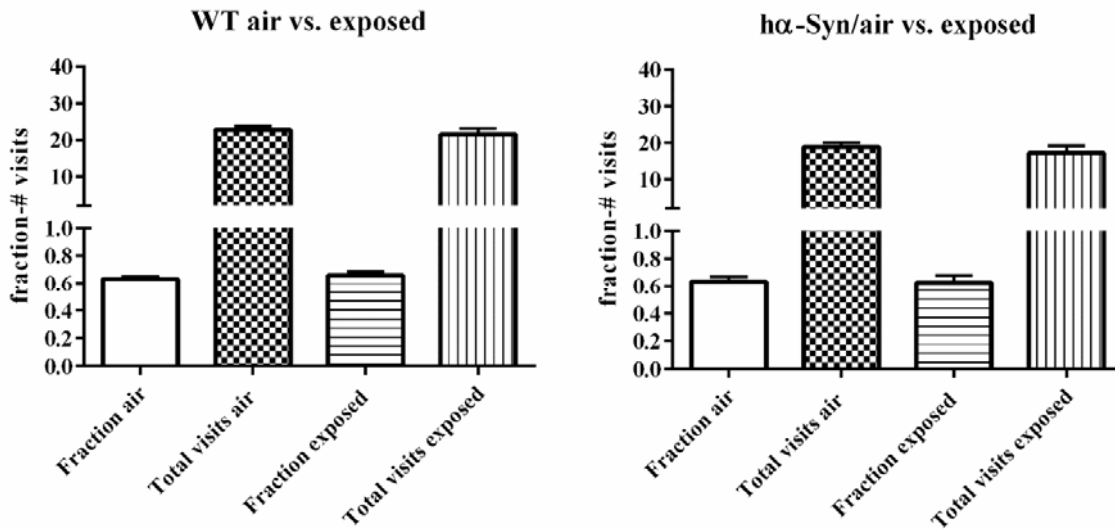


Figure 2.2.4 Y maze spontaneous alternations.

The Fraction represents the number of consecutive entries in three different arm) / total visits, and total number of visits into any of the three arms are shown (means \pm SEM; 16- 20 animals per group). Significant differences between groups \pm AP exposure were not observed, e.g., WT-Fraction air vs Fraction exposed; h α -Syn - Fraction air vs Fraction exposed (Student's t-test; $p > .05$). See Appendix 4 for statistical parameters.

Y-Maze – Results and Discussion

All groups showed similar results of $\sim 60\%$ for the percentage of alternations, i.e., consecutive entry in three different arms as a function of total visits. Those results are within the range of typical alternation rates, suggesting that the experimental methods factors did not mask any differences between groups. Although the septal-hippocampal system is crucially involved in spontaneous alternation, other brain areas are also involved, including the cerebellum, thalamus and substantia innominate; however, it appears that the neither the exposure conditions or increases in hippocampus h α -Syn expression that was subsequently measured (see Figure 2.3.6) affected performance in this test.

2.3 Task 3: Brain pathology assessments

2.3.1 Background

Multiple aspects of brain pathology that have been associated with PD and other neurodegenerative diseases were evaluated in both h α -Syn and wild type mice following the long term PM_{2.5} and filtered air exposure. Measures were obtained at 1 wk following the end of the 22

wks of exposure and included oxidative stress, neuroinflammation, and neurochemical levels of dopamine and norepinephrine. At the end of the exposure period for each cohort, the animals were sacrificed, the brains were collected and subsequently dissected (striatum, hippocampus, cortex) and frozen until time of analysis. The dissections of the brain regions were obtained bilaterally so that the tissues could be appropriately processed unilaterally for ELISA assays and neurotransmitter levels, respectively. To assess the pathological status of the brain following the exposure procedure, homogenates of the hippocampus and striatum from each animal were analyzed for the following biomarkers of PD-associated toxicity (Table 2.3.1).

Table 2.3.1 Neurochemical measurements of brain samples

Analyte	Marker function	Method
TNF α , IL-6	Inflammation	ELISA
HO-1	Adaptation/anti-inflammation	ELISA
human alpha-synuclein	Pathology development	ELISA
Hippocampus Norepinephrine	Neurotransmitter deficit	HPLC-ECD
Striatum Dopamine	Neurotransmitter deficit	HPLC-ECD

TNF α : tumor necrosis factor alpha; IL6: interleukin 6; HO-1: heme oxygenase-1; HPLC-ECD: High performance liquid chromatography-electrochemical detection

Methods - ELISAs

Brain tissues were weighed and homogenized in M-PER containing 150 mM NaCl, 1 mM PMSF and protease inhibitors using a Bioruptor System (3 cycles of 30 s on/30 s off, 320W) at 4°C. Samples were centrifuged at 14,000 x g for 20 min at 4°C. Protein levels were determined with a BCA Assay Kit. Supernatants were aliquoted to microcentrifuge tubes and stored at -65°C until analysis.

2.3.2 Results

Cytokine measurement/markers for cell status - TNF α recovery experiment.

As part of the validation of each analytical procedure used, we typically performed “recovery” experiments in which a known quantity of analyte was added to samples of the medium such as cell extract, media or tissue homogenate and subjected to the analytical protocol. Although solutions such as cell culture media, plasma typically present minimal recovery problems, cell or tissue homogenates are complex and can interfere with the analytical procedure. This problem is particularly important in tissue homogenates for they contain lipids, proteins and other complex

molecules that can trap or otherwise complex with protein analytes. We performed recovery experiments with TNF α and IL-6 and the nature of the experiment with TNF α and brain homogenate is shown below as an example. Thus, to brain homogenates of varying dilutions (1:2, 1:3, 1:4) was added the quantity of TNF α to a final concentration of 22 pg/mL and each dilution was analyzed following the protocol described by the ELISA kit supplier. The concentration of TNF α was determined and the recovery calculated from the quantity found as a percentage of the quantity actually added. The results of the experiment with each value as the average of three separate analyses are shown in Figure 2.3.1.

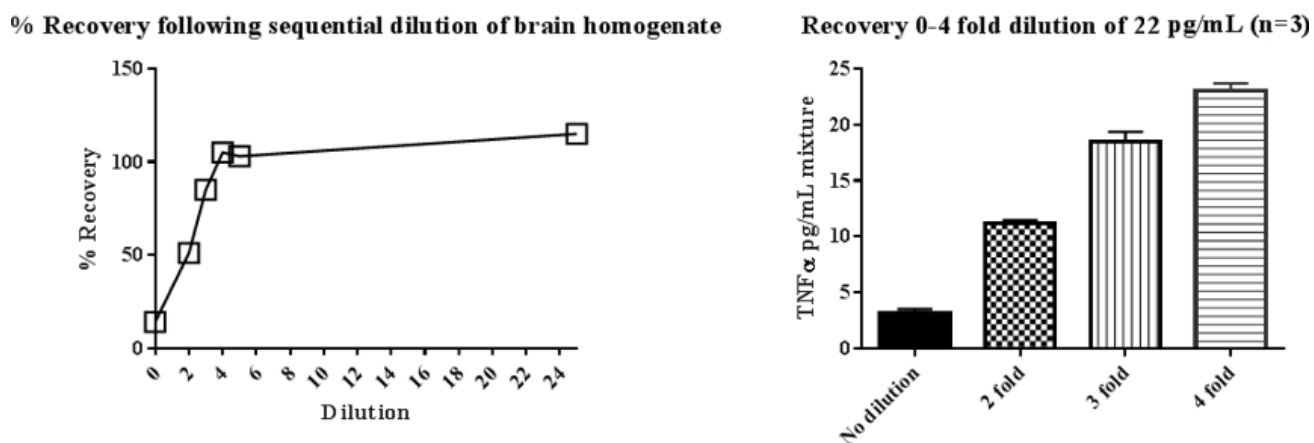


Figure 2.3.1 Recovery of TNF α from mouse brain homogenates.

The results showed that a minimum of a 1:4 dilution of the homogenate was required for recovery of added analyte. These results indicated that this dilution was required to insure an accurate analysis of TNF α . However, the dilution reduced the TNF α concentration in the sample and when 1:4 diluted brain homogenate samples were analyzed, we found that the TNF α levels were below the sensitivity of the assay procedure. Thus, we were unable to measure changes in TNF α brain levels.

Interleukin-6 (IL-6)

A similar problem was encountered with IL-6, in that brain levels were minimally detectable (but did show a trend towards significance). The initial analysis of individual hippocampus samples (14 animals) provided 1-5 mg protein per mL of homogenate. When subjected to the ELISA analysis for IL-6, the actual quantities of protein were close to the lower limit of the standard curve. The results from that analysis are provided in Figure 2.3.2 (left side).

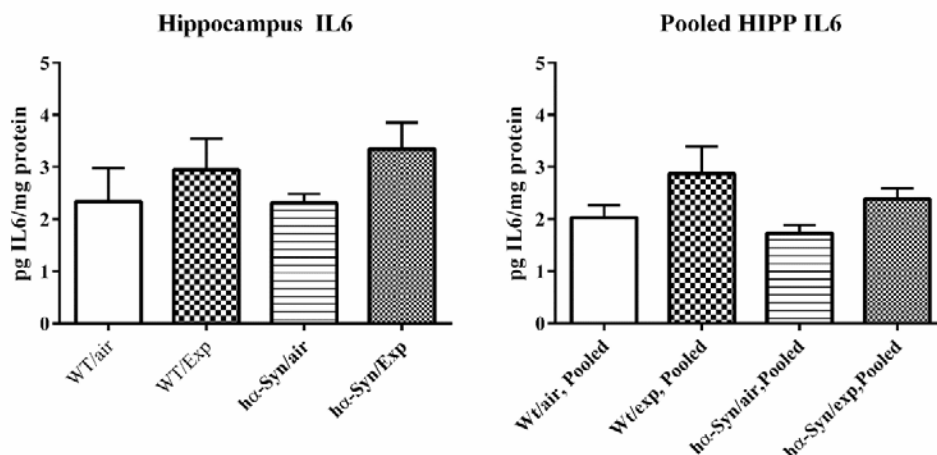


Figure 2.3.2. IL-6 levels in hippocampus.

Hippocampus content of IL-6 in WT and hα-Syn mice following exposure to ambient (filtered air) and concentrated (exp) PM_{2.5} are shown. The left panel summarizes analysis of individual tissues from 5 (wild type) and 14 hα-syn mice (means ± SEM). The right panel summarizes analysis of a 2nd group of pooled (5 mice in each group) tissues performed in duplicate. Differences between exposed & filtered air were not significant (Student's t-test; $p > .05$).

IL6 - Results and Discussion

To assess the significance of the differences in IL-6 at the low levels observed, a second analysis of pooled hippocampus samples from 6 mice of each group, generated by Centricon, based concentration was performed. Centricon allows the concentration of a dilute protein solution by a centrifugation based concentration; the pooled sample is centrifuged in a two compartment tube that allows the solute to filter while retaining the high molecular weight solutes. This procedure allowed the concentration of the analyte solution to increase from 1-5 mg protein/mL to 13-15 mg/mL. The results of the second analysis are shown in Figure 2.3.2 - right side. Overall, the results showed only trends of increases in the hα-Syn/Exp group vs the hα-Syn /Air that were consistently measured in the initial and pooled assays.

In their study of the effects of diesel exhaust particle (DEP) exposure on rats, Levesque et al. (Levesque et al. 2011) found significant increases in brain levels of IL-6, TNFα following exposure to 35-100 μg/m³ in their paradigm. The exposure used in our study was 90 ± 10 μg/m³ of concentrated ambient particles, so while total particle counts were comparable, we have found the prooxidant content per mass of the DEP (43 units/mg) to be considerably higher than ambient PM (7 units/mg). Although the actual exposure conditions used here were considerably lower in chemical activity than DEP, the exposure paradigm used in this study was derived from prevailing ambient air pollution levels in Southern California., albeit quantitatively lower to that in San Bernardino (see table 2.4.1).

Hemeoxygenase-1 (HO-1) results and discussion

An ELISA HO-1 assay had been previously described for mouse brain (Kitchin et al., 2001) in which levels of 7.7 ng/g tissue were measured.

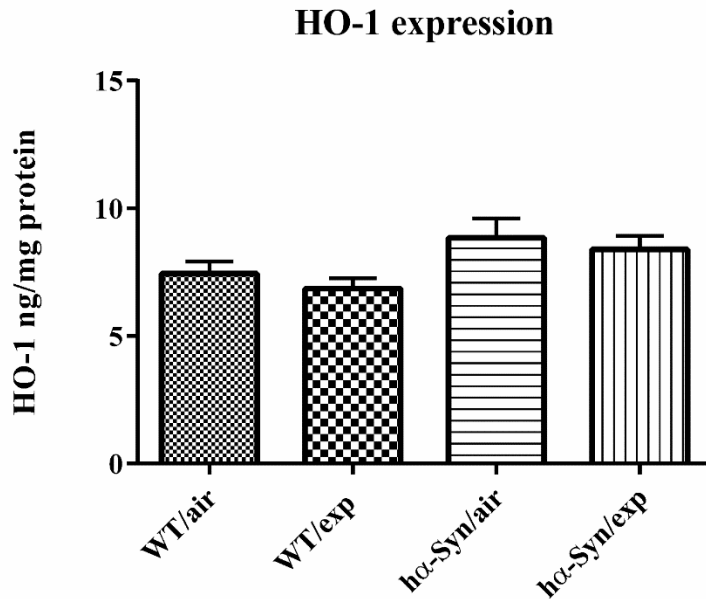


Figure 2.3.3 HO-1 levels in hippocampus.

The values shown are the means \pm SEM for 14 animals. The values were not significantly different (Student's *t*-test; $p > .05$).

Methods – DA/striatum and NE/hippocampus levels

The primary outcome measures were DA content in striatum and NE content in hippocampus because those analytes have been extensively used and validated as markers of neurotransmitter system integrity in those brain regions. DA and NE content was measured by HPLC-ED, using our published methods (Segal et al., 2005; Lacan et al., 2013); the values represent the analyte brain levels at 1 wk after the 22nd wk (i.e., last) AP exposure.

DA and NE Brain Content in Striatum and Hippocampus – Results and Discussion

Differences between exposed and filtered air were not significant at the $p < .05$ level as shown in Figure 2.3.4 and 2.3.5.

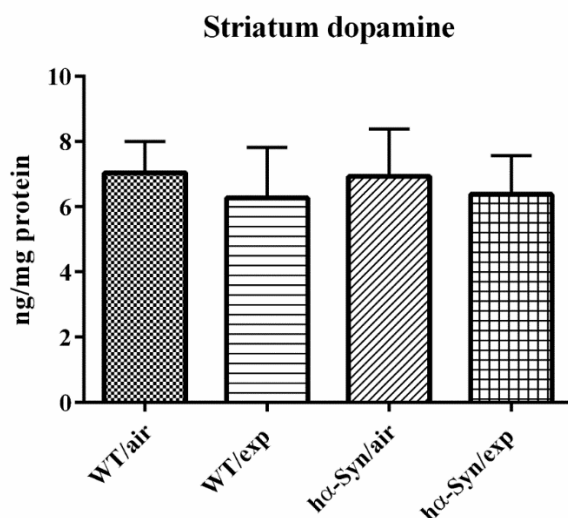


Figure 2.3.4 Striatum dopamine content.

Dopamine content in the striatum was measured in independent comparisons: *hα-Syn* ± AP, and wild type ± AP mice (means ± SEM for N of 12-15 per group). Comparisons ± AP were not significantly different (Student's *t*-test; $p > .05$). See Appendix 4 for statistical parameters.

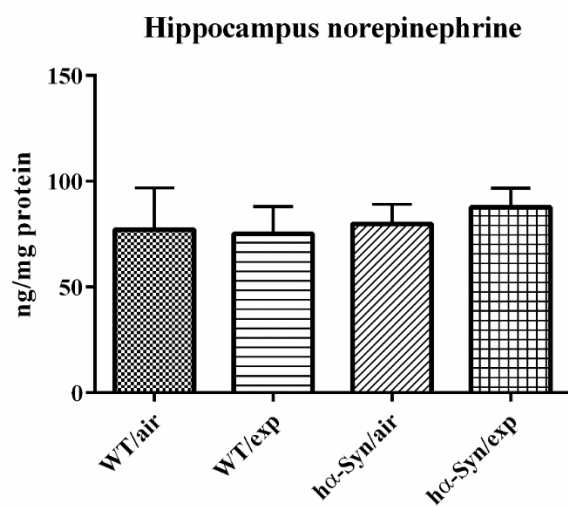


Figure 2.3.5 Hippocampus norepinephrine content.

Norepinephrine content in the hippocampus ($n = 12 -15$ per group). Values were not significantly different (Student's t -test; $p > .05$).

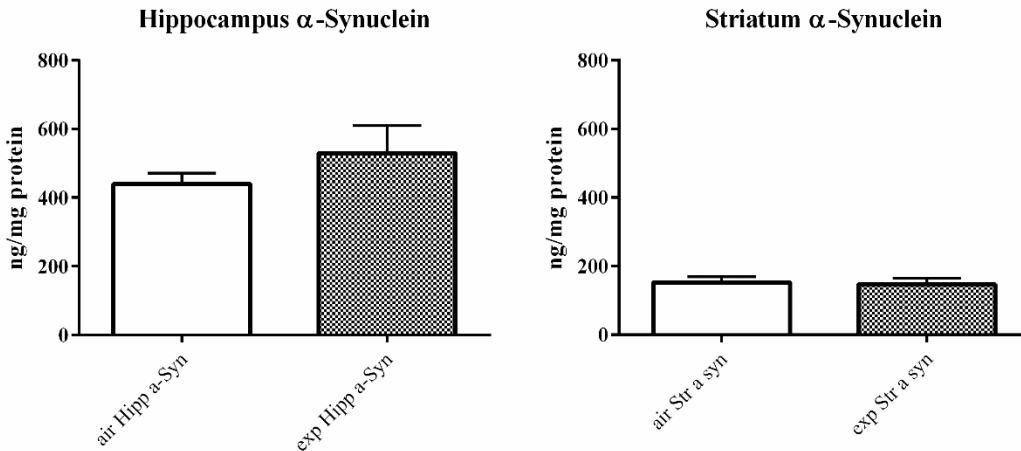


Figure 2.3.6 $h\alpha$ -Syn Content in Striatum and Hippocampus.

Study Result: No significant differences for $h\alpha$ -Syn protein levels in hippocampus were measured between air and AP-exposed $h\alpha$ -Syn mice (Student's t -test; $p > .05$).

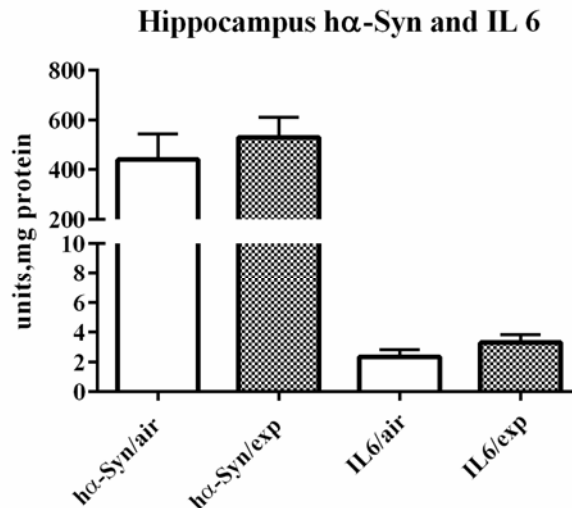


Figure 2.3.7 Summary of Hippocampus $h\alpha$ -Syn and IL-6 Content.

$h\alpha$ -Syn protein in the hippocampus for air and exposed $h\alpha$ -Syn mice.

Results and discussion

Although trends of an exposure effect were detected for post-exposure h α -Syn and IL-6 content in hippocampus, the differences were not significantly different at the $p < .05$ level.

Alpha synuclein exists in two states: a lipid-bound state on synaptic vesicles which mediates its normal function in the brain. “The common opinion in the field has been to view monomeric α -syn as the physiological, ‘healthy’ state of the protein and assign any observation of oligomeric α -syn to be pathological and relevant to the disease process”(Dettmer et al, 2016). Insoluble α -syn aggregates have been identified in PD but the soluble fraction appears to also form oligomers as shown by increases in post-mortem brain extracts from patients with dementia with Lewy bodies relative to controls (Paleologou et al. 2009). Also, detergent-soluble forms of α -syn have been associated with pathology of multiple system atrophy and dementia with Lewy bodies (Campbell et al. 2001).

Since it is not precisely known which form of α -syn is damaging to cells, all types of α -syn, not just those in inclusions, need to be investigated. Protein aggregation is associated with cell damage but whether aggregation itself is the key pathogenic event remains to be established. Accordingly, whether the increases in soluble α -syn we measured would subsequently transition to form oligomers remains an open question but, that said, a previous study using this same strain of h α -Syn mice measured age-dependent increases in total α -syn and those increases were associated with the development of motor deficits (Amschl et al. 2013).

2.4 Task 4: Chemical and biological characterization of PM

Introduction

The essential element of a study examining the potential health hazards of exposure is to have a quantitative description of both the exposure and of the health hazard being assessed. Such a description would provide a rigorous assessment of the findings and the possibility of extending the findings to other studies that have analogous results. Accordingly, wherever possible, we have collected quantitative data that describes what we believe are descriptors of the exposure and of the biological responses. In collecting these descriptors, however, we used in vitro assessments of the chemical and biological properties of the exposure media which for reasons discussed below, cannot be directly applied to an in vivo exposure. Nevertheless, we believe the in vitro based data are relevant to interpreting the results of in vivo responses by providing quantitative data on the exposure media. To explain the key differences between the in vitro and in vivo exposure, we summarize the toxicokinetics of exposure and the rationale for our approach to quantitative biological data collection.

2.4.1 Background

Toxicokinetics of AP exposure

A common in vitro exposure paradigm used to determine the potential toxicity of air pollutant mixtures is to use varying concentrations of sample and a prolonged exposure (up to 16 hours) to macrophage preparations. However, in a study examining the disposition of 1,4-benzoquinone (1,4-BQ) and 9,10-phenanthroquinone (9,10-PQ) with the murine macrophage cell line RAW 264.7, we have observed that these compounds are metabolized to inactive species in the preparation within 1 hour (unpublished observations). Studies with the A549 epithelial cells have shown that the prooxidant actions of 9,10-PQ are also terminated by conjugation with glucuronic acid (Taguchi, Shimada et al. 2008). This rapid change in concentration of the reactive organic species indicates that the observed effects are those that occur during the initial 1-3 hours and the changes observed after 16 hours may not be attributable to the initial offending chemicals. In other words, the resulting changes in cellular events most likely reflects actions associated with an acute interaction with cellular proteins followed by downstream cell events in response to these initial interactions.

In contrast, the actual human exposure to air pollutants is a continuous or steady-state process as the pollutants enter the lungs continuously with breathing. During this time period, although reactive chemical species could be inactivated, polynuclear aromatic hydrocarbons (PAH) could be processed by the enzymes mentioned above and converted to carcinogenic compounds which over time can begin to accumulate with the steady influx. Likewise, despite low concentrations and inactivation reactions, electrophiles can form covalent bonds with available nucleophiles and the resulting modified nucleophiles will accumulate in a manner that reflects the ratio of the turnover rate or half-life of the modified protein to the rate of entry of the electrophiles, into the biological system. Thus, both the effects of continuous AP exposure and covalent bond formation can result in a gradual accumulation of cellular responses that could be significantly different from those observed in acute models of AP exposure.

A second feature of real-life exposure is the rapid reaction of AP components with those of lung lining fluid, most notably ascorbate (Asc), which is present in the fluid at concentrations of 280 μM (Sun, Crissman et al. 2001). At this concentration, Asc will react with prooxidant metals and quinones to generate hydroxyl radical (see Figure 2.1.4) (Di Stefano, Eiguren-Fernandez et al. 2009) and initiate a lipid peroxidation reaction (Figure 1.1.3) (Araujo, Barajas et al. 2008). This reaction will also proceed continuously and at rates that reflect the concentrations of the incoming metal prooxidants and the availability of ascorbate. Although organic compounds are metabolized by phase I and II enzymes, the metal ion removal may occur at a much slower rate since it will be dependent on convection transport of the fluid itself.

The role of metals in AP toxicology also warrants a more systematic investigation. For example, humic-like substances found in particles form stable complexes with metals and these complexes have different physical-chemical properties from the metal ions themselves (Ghio, Stonehuerner et al. 1996, Davies, Ghabbor et al. 2001, Verma, Wang et al. 2015). These complexes may be able to penetrate membranes to gain access to the cell interior where they can dissociate. Most previous studies examining AP toxicity used organic extracts of particulates which may or may not have included the metals, or have used diesel exhaust particles known to contain high levels of organic matter. In actual exposure conditions, the complexes can be suspended in the lung lining fluid and the metal-organic complex could dissociate to allow the complexed redox active metal ions to react with ascorbate in the lung lining fluid.

The cellular targets affected by AP reactive species most likely reflect their access to the cell interior and rates of reactions with cellular targets relative to the rates of inactivation reactions. As these species enter cells by diffusion or by transport, they interact with protective biomolecules that reduce their potential impact. For example, although hydrogen peroxide generated extracellularly by prooxidant action can enter the cells, its concentration is carefully controlled by enzymes such as catalase, peroxyredoxin, and other reducing enzymes at diffusion controlled rates (Ferrer-Sueta, Manta et al. 2011). For this reason, the oxidation of thiols by intracellular peroxide must be a highly localized reaction in the cell. Additionally, organic prooxidants such as polyhydroxy aromatic compounds are inactivated by ester-forming conjugation reactions (Taguchi, Shimada et al. 2008) and organic electrophiles are inactivated by conjugation with the cellular nucleophile, glutathione (Prester, Zhang et al. 1993), thus, limiting their cellular persistence. Nevertheless, in spite of these inactivating processes some electrophiles do interact with available thiolates. Here, it should be pointed out that the reaction between electrophiles and nucleophiles such as thiols involves the ionized thiolate form of the thiol (Figure 1.1.3). Thus, the critical concentration is that of the thiolate, not the thiol; further, the thiolate concentration depends on the intracellular H^+ concentration and the pKa of the thiol. The pKa values of thiols in proteins such as GAPDH, PTP1B and Keap1 are lower (~ 5) than that of a typical thiol such as cysteine and glutathione (~ 9). Thus, in spite of the low concentration of the protein itself, the concentrations of the potentially toxic thiolate or nucleophile functions can be comparable to that of protective low molecular weight thiols such as glutathione.

Cellular responses

Two general cellular responses to these reactive species can occur: adaptation (Gozzelino, Jeney et al. 2009) which protects the cell by inactivating the offending species, and inflammation which triggers cellular events that are negatively associated with exacerbation of asthma and other diseases and positively associated with protection against microorganisms and limitation of cancer growth (Park, Kim et al. 2009, Ribeiro, Freitas et al. 2015, Mostofa, Punganuru et al. 2017). The adaptive response, also referred to as an anti-inflammatory response, acts in opposition to the proinflammatory response. These responses are mediated by distinct pathways and as for most

biological responses are dependent on the concentration of the triggering agent(s). It should also be pointed out that both anti- and proinflammatory responses can be considered adverse health responses. For example, the anti-inflammatory response can increase organism sensitivity to microbial attack by suppressing the immune response and the resulting inflammation can result in exacerbation of chronic diseases such as asthma and atherosclerosis through increased expression of cytokines. The anti-inflammatory response can also promote carcinogenesis by inhibiting cancer cell growth regulation by the inflammatory processes. Thus, the cellular effects of AP mixtures can be viewed as a balance between anti- and proinflammatory responses. This notion, simplistically summarized in Figure 2.4.1 represents the basis for our cell response studies.

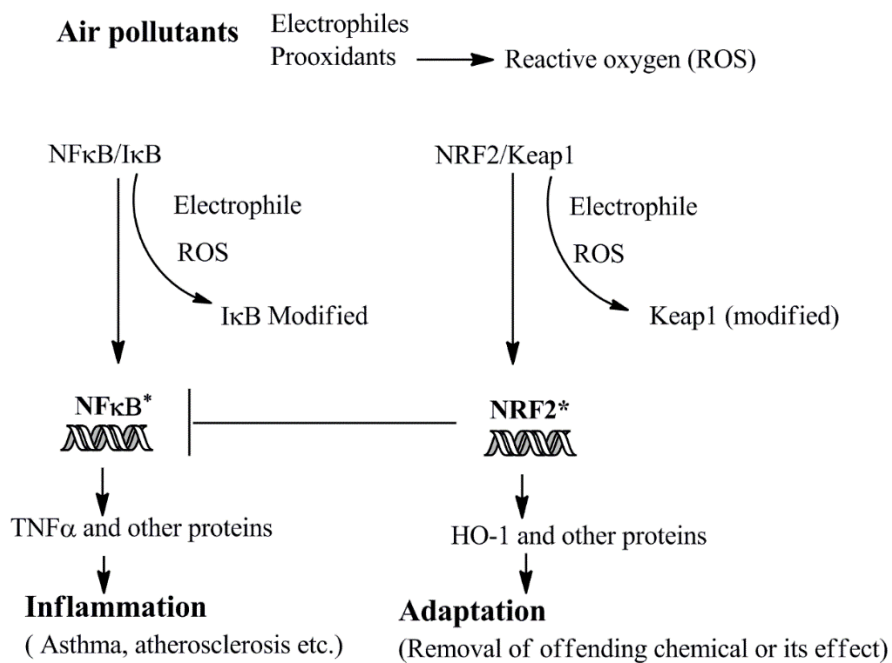


Figure 2.4.1 Air pollutants and their cellular targets.

Two cellular signaling cascades, a pro-inflammatory cascade, mediated by the transcription factor NFκB and an adaptive, or anti-inflammatory cascade with Nrf2 as the transcription factor are shown. These cascades have a 'ying-yang' relationship in that the adaptive response antagonizes the inflammatory response, shown by the line inhibiting NFκB activation. In the resting state, the transcription factors are complexed with inhibitory regulators which dissociate upon reaction with electrophiles or reactive oxygen species (ROS) generated by the prooxidants of the pollutant mixture. The result of the activation can be inflammation or adaptation, depending on the concentrations and nature of the offending chemical mixture. The line between Nrf2 and NFκB is meant to indicate an antagonistic relationship between the actions of the two factors.

In this scheme, the cytokine, $\text{TNF}\alpha$ is a marker for activation of $\text{NF}\kappa\text{B}$ - a transcription factor associated with the inflammatory response, and the antioxidant enzyme, HO-1 is a marker for Nrf2 activation - the transcription factor associated with anti-inflammatory, adaptive responses. The expression of these two markers then reflects the status of the cell as it responds to the insults caused by the reactive species in air pollution. We have used LPS as an inflammatory stimulant and a J-DEP investigators as a HO-1 stimulant to serve as standards for the actions of increases in $\text{TNF}\alpha$ and HO-1 levels with increasing concentrations of LPS and J-DEP.

In a chemical perspective of this model of cell response, ROS, most notably hydrogen peroxide, generated by prooxidant action, oxidizes cysteine thiols to sulfenic acids, causing the breakdown of inactive complexes of transcription factors to their active forms (indicated by the asterisks in Figure 2.4.1). Alternatively, electrophiles react with electron rich functionalities such as cysteine thiolate and lysine amino groups of proteins to form irreversible covalent bonds (Dinkova-Kostova and Talalay 2008, Iwamoto, Nishiyama et al. 2010, Jacobs and Marnett 2010). Thus, electrophiles can modify the same thiols as those affected by hydrogen peroxide and dissociate the transcription factor complex to allow the transcription factor complex to dissociate. The relevant transcription factors, $\text{NF}\kappa\text{B}$ and Nrf2, then enter the nucleus and stimulate expression of multiple proteins including the two marker proteins, $\text{TNF}\alpha$ and HO-1, respectively. The relative quantities of the two proteins reflects the activation status of the inflammatory events.

This model of pro- and anti-inflammatory events was derived from a previous study of the cellular effects of coarse particle samples that were collected in the Basin and examined by our laboratory and Dr. Ning Li for their chemical and cellular responses. In that study, a high correlation was observed for $\text{TNF}\alpha$ and IL-6 and MCP, all pro-inflammatory markers, and with organic carbon content but not with water-soluble iron or copper. The correlative factor for the proinflammatory response was organic carbon content, but not DTT activity. In her original study of DEP with macrophages, Dr. Li (Li, Venkatesan et al. 2000) reported a high correlation between organic carbon and the expression of HO-1, and a subsequent study showed a high correlation between organic DTT and HO-1 expression levels (Li, Sioutas et al. 2003). Although these data suggest that the AP components most closely linked to cellular responses are organic compounds, it does not exclude metals for their effects that may depend on the organic-metal complexes described above for humic-like substances.

Quantitative analyses of biological responses: The concentration-response curve

In order to utilize the chemical assays above in interpreting the cellular actions of the particles, biological responses must also be quantitative, i.e., reflecting the potency of the sample in the response measured. In chemical reactions, a linear relationship between concentration and rate is

assumed because that is usually observed but biological responses are, in fact, not always linear. There are three reasons for non-linearity of biological responses. One is saturability; typically a concentration vs. response relationship with a biological stimulant is saturable, i.e., the relationship reaches a maximum beyond which increasing concentration does not further increase response. A second reason is the resting or control state. Cells and therefore organisms in general maintain their components in an approximate steady-state by continuous synthesis and degradation. When challenged by external events or chemicals, the cell responds by altering the steady state concentration of these components to a new steady-state. The concentration of a monitored biomolecule in this new steady-state can be higher or lower than that of the control and, if lower, a negative slope for the stimulus concentration vs. response curve results. The third reason is hormesis which is the notion of a net response that is the result of two opposing responses such that the observed response can be initially positive and subsequently negative, depending on the concentrations used. As these changes are concentration-dependent, the concentration-response curve comparing changes relative to a control state can have a positive or negative slope, or if over a wide concentration range a “U” shaped concentration-response curve.

Requirement for a linear relationship between exposure concentration and biological response

Due to these varying concentration-response relationships, we maintain that all quantitative cell experiments should be performed with different exposure concentrations to generate concentration-response curves, using the slopes and intercepts as measures of the potency or efficacy of the sample. The use of linear regression procedures to estimate slopes provides a statistical approach to assess the validity of the concentration dependency of the slope and its positive or negative value. The rationale for a linear relationship of data generated in these AP dependent cell responses, which are very different from those reflecting a specific effect such as that from botulinum toxin is described below:

In pharmacology and toxicology, the relationship between a dose of toxin or drug and its physiological response is represented by the logistic function,

$$\text{Effect} = a \cdot M / (a + K^n)$$

where “a” is the concentration of the stimulus, “M”, the maximal value obtained and “K” a constant reflecting the affinity of the stimulant to its target and “n” is a stoichiometric factor applicable to a specific interaction. This relationship is a curvilinear one, typically exhibiting saturation when $a \gg K$. However, if one examines effect under conditions where $a < K$ (a is a small number compared to K because of the non-specificity of the interaction), and $n = 1$, the expression becomes

$$\text{Effect} = a \cdot (M/K),$$

a linear expression, relating the effect to concentration of sample times a constant (M/K) that reflects the potency of the sample and its maximal effect.

The responses being measured in air pollution studies are due to an unspecified mixture of active species, so “a” becomes a measure of the concentration of the mixture whose action should be dependent on its concentration.

Then, the response such as expression of TNF α is defined as the effect,

$$\text{Effect} = [a] * \text{Slope}$$

$$\text{Slope} = (\Sigma \text{ concentrations of reactive species}) * (\text{their intrinsic biological activity})$$

where “a” is the concentration of the sample in the culture media.

A plot of varying volumes of air pollutant mixtures per mL (a/mL) of media vs. biological response (ng protein/mL or mg protein) should be linear with the slope as a measure of sample biological activity. With the chemical rationale in section 1.1 and this biological perspective we have examined ambient air samples collected at the Irvine exposure site and compared the results with those from other sites in the Los Angeles Basin. With these considerations in mind, we have compared the results of our characterization of the exposure media in Irvine with one involving ambient air samples collected in the LA Basin using the same collection techniques as well as chemical and biological analytical procedures.

2.4.2 Results

Chemical and cellular properties of Irvine air pollutants in Irvine and a comparison with other sites in the Los Angeles Basin.

Chemical properties

Figure 2.4.2 compares the chemical properties of the Irvine ambient air samples (UCI) with those collected in the SCAQMD study of communities neighboring railyards in Commerce (CM), Long Beach (LB) and San Bernardino (SB) and 4 additional sites in Commerce (CMA, CMB, CME and CMf). Sites CM, LB and SB refer to sampling sites within a 1 mile radius of the respective railyard, and the CMA to CMf sites were at different locations near the CM railyard, with CMA and CMB in close proximity (~1 mi), CME, a background site about 2 miles upwind from the railyard and CMf a diesel truck loading area. Comparing the two sets of samples, it is noteworthy that although the PMDTT values exhibit activities in the same range, the addition of DTPA to PM only partially blocked activities of the UCI samples while essentially completely blocking the SCAQMD activities. Since the metal chelator, diethylenetriamine pentaacetic acid (DTPA), blocks metal based DTT activity (see for example, (Di Stefano, Eiguren-Fernandez et al. 2009)), the UCI samples appear to have significant non-metal prooxidants such as hydroquinones and other redox active organic compounds compared to the SCAQMD railyard sites. A comparison of the XAD or vapor samples from the two studies indicated a lower GAPDH activity in the UCI samples. In summary, the Irvine samples have higher levels of organic prooxidants in the particle phase with lower levels of organic electrophiles in the vapor phase than the Los Angeles Basin Railyard sites.

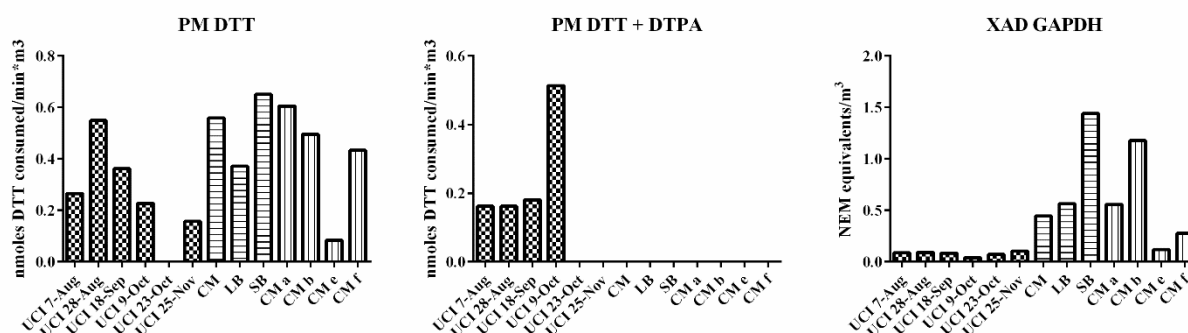


Figure 2.4.2 Reactive components of ambient air in Irvine (UCI) and other sites in the Los Angeles Basin.

Ambient air samples were collected in communities neighboring railyards in Commerce (CM), Long Beach (LB) and San Bernardino (SB) using published procedures (Eiguren-Fernandez 2015). The sites labeled CMA, CMB, CMe and CMf refer to samples collected in Commerce at distances less than 1 mile from a railyard (a, b), a site upwind and about 1 mile from a railyard used as a background site (e) and a diesel truck parking site (d) also distal from a railyard.

Table 2.4.1. Comparison of PM prooxidant properties

City	Average PM DTT	Average PM DTT + DTPA	% non metal DTT
Beijing	3.5	0.19	5%
Mexico City	3.3	0.63	19%
Los Angeles (110 Frwy)	2.5 (Verma, Pakbin et al. 2011)	NA	NA
San Bernardino	0.65	0.00	0
Irvine	0.23	0.081	35%
Irvine times 12	2.76	0.97	

Table 2.4.1 compares the prooxidant content and properties of the Irvine samples with those from Beijing and Mexico City, as well as those from San Bernardino, CA. All of the analyses have been performed by the same protocols and should be directly comparable. The Beijing and Mexico City samples were collected in 2017 and 2009, respectively. Also included is a value from a sample collected along the 110 freeway in Los Angeles during 2011. The Irvine samples were the least active and about 1/10 that of samples collected adjacent to the 110 freeway. The

Irvine sample also contained higher levels of organic prooxidants than found in other samples. This limited sampling from different locations demonstrates the wide variation in prooxidant content and also shows qualitative differences in their nature, i.e., with respect to organic prooxidant content.

Cellular (in vitro) responses to Irvine vapor phase components

We encountered two problems with the cell experiments, a technical one and a laboratory one. In the first case, limited quantities of each sample prevented a concentration dependent study so a single concentration cell experiment was performed using an air equivalent of 3 m³/mL cell media in triplicate. Although this approach compromised our earlier requirement of a concentration-response regression slope, the varying levels of prooxidants each vapor sample provided a dose-response of sorts. Secondly, a reconstruction of the cell culture facility available to us limited its access and we were unable to perform a particle-cell study; the only cell study accomplished was with the vapor phase of ambient Irvine air. Thus, the effects of the vapor phase samples on expression of HO-1 (adaptation/anti-inflammation) and TNF α (inflammation) by Raw 264.7 mouse macrophage cells were determined by exposure to a DMSO solution of the dichloromethane extract of the XAD resin (vapors) at an air volume equivalent concentration of 3.0 m³/m media. A DMSO blank, whose volume corresponded to the vapor sample, was used as a control. The cells were cultured for 16 hours, the medium and cells separated and the cells subjected to lysis to obtain a cell extract. The cell extracts were used in the ELISA assays for HO-1 and the medium used to assay TNF α using instructions provided by the manufacturers (HO-1; Enzo Life Sciences; TNF α , BD Pharmingen). The results are shown in figure 2.4.3 as a plot relating expressions of the two proteins.

Results of cellular exposure to Irvine vapor phase samples

The Irvine samples stimulated HO-1 expression relative to a DMSO blank while TNF α levels were lower than those of the DMSO blank and when plotted against each other (figure 2.4.3) a negative line relating the two results.

TNF α and HO-1 expression following exposure to vapor phase components

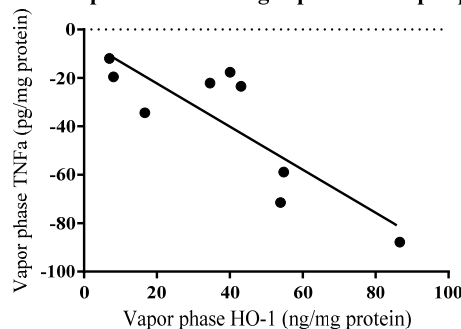


Figure 2.4.3. Expression levels of HO-1 and TNF α following stimulation by vapor phase components from Irvine collections.

The analyte concentrations are from the cell extract (HO-1) and media (TNF α) following stimulation of Raw cells with vapor phase extracts at a fixed concentration of 3 m³/mL. The negative TNF α values reflect a suppression of expression relative to the DMSO control. The line is the regression of the data which has a slope of -0.88 ± 0.2 with a r^2 value of 0.70.

The positive HO-1 responses (the X axis) observed reflect an anti-inflammatory property of the samples at these concentrations which resulted in suppression of TNF α expression (see figure 2.4.1).

Relationship between chemical properties and cellular effects

The quantitative nature of the data (table 2.4.2) allows assessment of the relationship between the determinations and we utilized Pearson analysis (table 2.4.3) for this purpose.

Table 2.4.2 Summary of chemical and biological properties of ambient Irvine PM_{2.5} and vapors.

Week	PM DTT	PM DTT (DTPA)	vapor DTT	vapor GAPDH	vapor HO-1	vapor TNF α	OC content
2	0.265	0.162	0.102	0.088	86.620	-87.770	1.64
6	0.549	0.180	0.009	0.093	53.920	-71.440	5.94
9	0.362	0.174	0.025	0.084	54.820	-58.850	9.85
13	0.138	0.019	0.008	0.036	40.090	-17.650	6.6
14	0.228	0.514	0.016	0.041	16.720	-34.390	18.26
15	0.073	0.000	0.026	0.055	6.990	-11.970	20.69
17	0.181	0.037	0.022	0.032	34.570	-22.130	16.75
21	0.156	0.000	0.016	0.103	8.070	-19.530	18.05
22	0.300	0.016	0.020	0.077	43.090	-23.440	8.06

Units for the chemical assays are expressed per m³. The cellular assay results are expressed as ng HO-1 per mg protein and pg TNF α /mg protein for a vapor sample concentration of 3 m³ per mL media. The negative value for TNF α expression indicates the addition of sample suppressed the control expression following cell stimulation by sample free DMSO.

Table 2.4.3 Pearson analysis of chemical and cellular data from Irvine.

The data of table 2.4.2 were subjected to Pearson analysis. Coefficients and their respective p values are shown with bold numbers indicating a significant ($p < 0.05$) correlation.

		Vapor HO-1	Vapor TNF α)	PM DTT	PM DTT (DTPA)	DTPA sensitive DTT	Vapor GAPDH	Vapor DTT	OC $\mu\text{g}/\text{m}^3$
Vapor HO-1	Coeff		-0.837	0.561	0.070	0.378	0.303	0.654	-0.913
	<i>P</i> value		0.005	0.116	0.859	0.316	0.428	0.056	0.001
Vapor TNF α	Coeff	-0.837		-	-0.388	-0.206	-0.519	-0.626	0.698
	<i>P</i> value	0.005		0.031	0.303	0.595	0.152	0.072	0.036
PM DTT	Coeff	0.561	-0.713		0.319	0.496	0.511	-0.028	-0.566
	<i>P</i> value	0.116	0.031		0.403	0.175	0.160	0.944	0.112
PM DTT (DTPA)	Coeff	0.070	-0.388	0.319		-0.665	-0.134	0.056	0.039
	<i>P</i> value	0.859	0.303	0.403		0.050	0.731	0.887	0.921
Vapor GAPDH	Coeff	0.303	-0.519	0.511	-0.134	0.525		0.269	-0.341
	<i>P</i> value	0.428	0.152	0.160	0.731	0.147		0.484	0.369
Vapor DTT	Coeff	0.654	-0.626	0.028	0.056	-0.073	0.269		-0.450
	<i>P</i> value	0.056	0.072	0.944	0.887	0.852	0.484		0.225
OC $\mu\text{g}/\text{m}^3$	Coeff	-0.913	0.698	-	0.039	-0.481	-0.341	-0.450	
	<i>P</i> value	0.001	0.036	0.112	0.921	0.189	0.369	0.225	

As stated earlier, we were unable to perform cellular particle studies because of laboratory modifications to the cell culture facility. However, in view of the high organic prooxidant content of the particle phase (see table 2.4.2), we felt that the cellular properties of VOCs which are in steady state equilibrium with the particles would be indicative of particle properties. Somewhat unexpectedly, the dominant chemical property correlating with the cellular response was particle prooxidant content (table 2.4.3). Thus, particle DTT activity showed an inverse correlation with TNF α expression which was negatively correlated with HO-1 expression. The negative correlation between HO-1 and TNF α is consistent with the notion of anti- and pro-inflammatory responses (see figure 2.4.1) and the positive relationship of HO-1 expression to prooxidant content, although not a significant correlation here, has been observed before (Li, Sioutas et al. 2003). The organic carbon content of the PM showed high correlation with the cell responses as well and when plotted against the cell responses, a linear relationship is observed (figure 2.4.4)

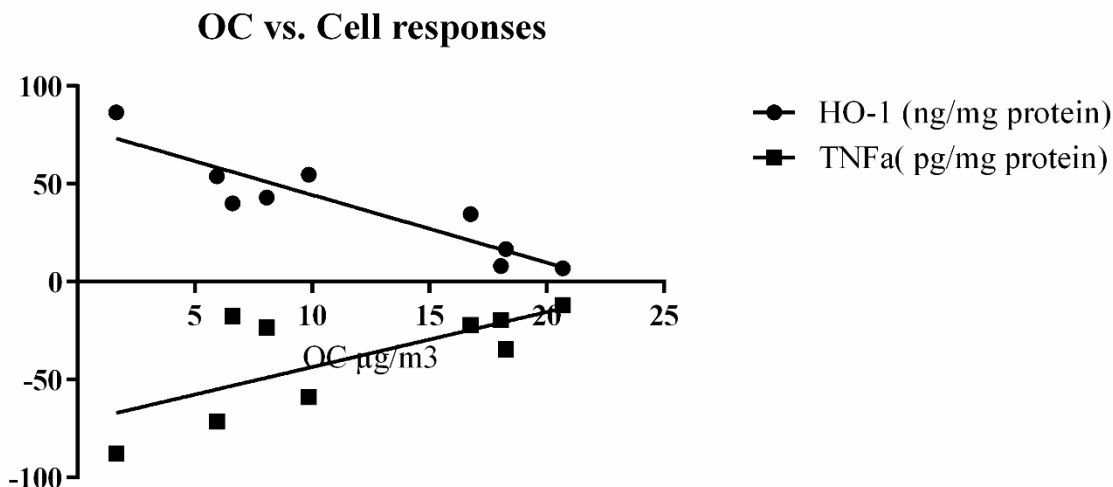


Figure 2.4.4 Organic carbon (OC) content vs. cell responses; Irvine samples

The organic carbon content of each sample is plotted against the expression of HO-1 and TNF α by Raw cells exposed to 3 m³/mL media. The lines represent the regression of OC vs. the respective cell response. The R squared values of the regression were 0.83 (HO-1) and 0.49 (TNF α). The values are net values or the difference between the response due to the vapor phase sample and that from the DMSO solvent. Thus, the negative TNF α response indicates the expression was lower than that due to the solvent alone.

The relationship between OC and cell response is of interest because OC has been measured in other in vivo studies using the VACES (see table 2.5.2) and can thus provide a means of comparison of this and other in vivo studies. The data of figure 2.4.4 indicates that as OC increases in the samples, the expression of TNF α increases with OC content from a level lower than that of control until at 20 µg/m³, expression approximates the control or DMSO based stimulation. Changes in HO-1 expression are the reverse, i.e., expression decreases with increasing OC content consistent with the opposing interactions shown in figure 2.4.1.

Comparison of Irvine cellular and chemical data with those of the SCAQMD railyard studies

To provide more context for the cellular and chemical data, the Irvine results were then compared with those from the SCAQMD railyard study, as the collections and analyses use the same procedures. The corresponding values for the SCAQMD study are shown in tables 2.4.4 and 2.4.5.

It should be pointed out that the precision of the SCAQMD cellular response data differ from those of this CARB study because of the rationale described in p 42-43 and practical reasons

cited on p 45. In summary, as stated in the legend of table 2.4.4, the values for cellular response are the slopes of a regression analysis of at expression data from exposure of cells to at least three concentrations in triplicate, while the cellular data of table 2.4.2 are the result of a single concentration ($3 \text{ m}^3/\text{mL}$) in triplicate and therefore assumes a linear concentration dependency of the observed responses. We felt justified in making this assumption because the SCAQMD data are from different geographical locations whereas the Irvine samples are all from the same site.

Table 2.4.4 Summary of chemical and biological properties of SCAQMD Railyard PM_{2.5} and vapors

	<u>PM</u> <u>DTT</u>	<u>PM</u> <u>GAPDH</u>	<u>PM</u> <u>DHBA</u>	<u>vapor</u> <u>DTT</u>	<u>vapor</u> <u>GAPDH</u>	<u>TNFa</u> <u>PM net</u> <u>slope</u>	<u>PM</u> <u>HO-1</u> <u>Slope</u>	<u>vapor</u> <u>HO-1</u> <u>Slope</u>
CM	0.559	0.033	0.379	0.066	0.444	5.56	5.25	34.49
LB	0.371	0	0.606	0.083	0.564	0	0	43.23
SB	0.651	0.011	0.477	0.149	1.44	392.02	80.3	182.4
CMa	0.606	0.116		0.038	0.557	19.64	4.83	21.05
CMb	0.496	0.122		0.101	1.178	19.33	0	47.74
CMe	0.084	0		0.021	0.119	0	0	0
CMf	0.433	0.043		0.038	0.277	0	9.55	12.19

The units for the chemical assays are expressed as units/m³. The cellular responses are the slopes of concentration response curves calculated from exposures data from triplicate values at 3 concentrations. Units are pg TNFa/mg protein per m³per mL or ng HO-1/mg protein per m³per mL. Net slope refers to the observed slope for the sample less corrections for blank filters and endotoxin levels.

As an addendum, we include table 2.4.4A, a comparison of the vapor phase properties, in which all values have been normalized to 3 m^3 , the concentration used in for the cell studies of the Irvine samples (Table 2.4.2). Note that the values for the SCAQMD sites are substantially higher, reflecting their proximity to railyards except for sites in Commerce (CMe and CMf) which were at least 1 mile from a railyard.

Table 2.4.4A. Comparison of the vapor phase properties from Irvine and other Los Angeles Basin sites at 3 m^3 .

Irvine (week)	Vapor GAPDH	Vapor HO-1	SCAQMD (Site)	Vapor GAPDH	Vapor HO-1
2	0.264	86.62	CM	1.332	103.47
6	0.279	53.92	LB	1.692	129.69
9	0.252	54.82	SB	4.32	547.2
13	0.108	40.09	CMa	1.671	63.15
14	0.123	16.72	CMb	3.534	143.22

15	0.165	6.99	CMe	0.357	0
17	0.096	34.57	CMf	0.831	36.57
21	0.309	8.07			
22	0.231	43.09			
22	0.231	43.09			

The values for the data shown are expressed per 3 m³. The electrophile content (GAPDH) and the HO-1 expression levels for the SCAQMD sites have been multiplied by 3 to allow direct comparison with the observed Vapor HO-1 values from the Irvine samples.

The correlation results for the SCAQMD samples are shown in table 2.4.5. In contrast to the Irvine samples (Table 2.4.3), however, HO-1 expression by the vapor phase SCAQMD samples appears to correlate with the corresponding vapor phase components (see comparison on table 2.4.6).

Table 2.4.5 Pearson correlation analysis of SCAQMD Railyard PM_{2.5} and vapors

The data of table 2.4.4 were subjected to Pearson correlation analysis. The bold numbers indicate a significant ($p < 0.05$) correlation

		<u>TNFa</u> <u>PM net</u> <u>slope</u>	<u>PM</u> <u>DTT</u>	<u>PM</u> <u>DHBA</u>	<u>vapor</u> <u>HO-1</u> <u>Slopes</u>	<u>vapor</u> <u>DTT</u>	<u>vapor</u> <u>GAPDH</u>	<u>PM</u> <u>HO-1</u> <u>Slopes</u>
TNFa PM net slope	Coeff		0.481	0.383	0.966	0.787	0.751	0.990
	P value		0.275	0.396	0.000	0.036	0.052	0.000
PM DTT	Coeff	0.481		0.468	0.567	0.576	0.642	0.493
	P value	0.275		0.290	0.185	0.176	0.120	0.260
PM DHBA	Coeff	0.383	0.468		0.536	0.587	0.364	0.383
	P value	0.396	0.290		0.215	0.166	0.422	0.397
vapor HO-1 Slopes	Coeff	0.966	0.567	0.536		0.915	0.852	0.942
	P value	0.000	0.185	0.215		0.004	0.015	0.001
vapor DTT	Coeff	0.787	0.576	0.587	0.915		0.934	0.739
	P value	0.036	0.176	0.166	0.004		0.002	0.058
vapor GAPDH	Coeff	0.751	0.642	0.364	0.852	0.934		0.686
	P value	0.052	0.120	0.422	0.015	0.002		0.089
PM HO-1 Slopes	Coeff	0.990	0.493	0.383	0.942	0.739	0.686	
	P value	0.000	0.260	0.397	0.001	0.058	0.089	

Samples from San Bernardino in the SCAQMD collections exhibited substantially higher levels of HO-1 inducing capacity and when it was deleted from the data set, a clear regression ($r^2 = 0.94$) was observed between the vapor prooxidants and the HO-1 response (Figure 2.4.5).

Analogous plot for the Irvine samples is also shown plotting the PM prooxidant content against cell responses.



Figure 2.4.5 Cell responses to vapor phase components plotted against correlated prooxidant assays.

The expression of HO-1 and TNF α (Irvine only; vapor phase components from the Railyard communities had no significant effect on TNF α expression) by Raw cells stimulated by vapor phase components in DMSO according to published procedures (Li, Alam et al. 2004). The values are net values after subtraction of the control (DMSO added to media) values. The negative values for TNF α expression reflect a suppression of the control DMSO response.

Table 2.4.6 Comparison of Pearson correlation results from Irvine and SCAQMD Railyard sites

<u>parameter 1</u>	<u>Parameter 2</u>		<u>Irvine</u>	<u>SCAQMD study</u>
Vapor HO-1	Vapor TNF α	coefficient	-0.837	ND
		P Value	0.005	ND
Vapor TNF α	PM DTT	coefficient	-0.713	TNF α not significant
		P Value	0.031	TNF α not significant
Vapor HO-1	PM DTT	coefficient	0.561	0.561
		P Value	0.116	0.185
Vapor HO-1	Vapor GAPDH	coefficient	0.303	0.852
		P Value	0.428	0.015
Vapor HO-1	Vapor DTT	coefficient	0.654	0.915
		P Value	0.056	0.004
Vapor DTT	Vapor GAPDH	coefficient	0.269	0.934
		P Value	0.484	0.002

Comparison of Pearson analysis results (Table 2.4.6) show the differences in the nature of the components associated with a common biological response, HO-1 expression, stimulated by vapor phase components. Thus, the stimulation of this anti-inflammatory marker was highly correlated with the vapor phase prooxidant and electrophile content of the SCAQMD Railyard samples whereas only the Irvine particle prooxidants correlated with this response. The organic carbon (OC) content of Irvine particles were highly correlated with the Irvine vapor phase HO-1 response (Table 2.4.3) suggesting organic compounds are involved.

In summary, the quantitative nature of the chemical and biological responses allowed comparison of data from multiple Los Angeles Basin sites and although the two data sets reflect different times, they indicate the samples from Irvine exhibited different characteristics from those in the SCAQMD funded study of communities near railyards.

2.5 Summary and general discussion.

2.5.1 Review of the *in vivo* and *in vitro* aspects of the project.

In response to a very helpful comment by a reviewer, we present here (Table 2.5.1) a summary of the project in terms of the *in vivo* and *in vitro* paradigms employed the *in vivo* exposure to CAPS and the *in vitro* exposure to the corresponding ambient PM_{2.5} water suspensions and DMSO solution of the VOCs trapped by a XAD resin.

The study was designed to test the notion that reactive chemicals in AP mixtures could exacerbate the progression of PD by inducing chemical stresses that initiate adverse cell responses such as inflammation. The project used an established paradigm for the disease and assessed whether exposure to concentrated UFPM of <0.18 (CAPS) would cause discernible changes in the transgenic animals. To characterize the exposure atmosphere, the ambient air PM_{2.5} and corresponding vapors were collected and subjected to chemical and cellular analyses.

Table 2.5.1 Comparison of *in vivo* and *in vitro* studies

In vivo (VACES-CAPS)	In vitro (PM _{2.5} and VOCs)
Protocols	
Two strains of mice were exposed to the VACES generated atmosphere, wild type and human α -synuclein expressing transgenic animals after which they were subjected to series of behavior tests assessing neurological	The <i>in vitro</i> studies utilized exposures of a murine macrophage cell line to the ambient particles as aqueous suspensions or DMSO solutions of concentrated vapor phase components after which pro-and anti-

deficits followed by neurochemical and inflammatory analyses.	inflammatory responses assessed by HO-1 and TNF α expression.
Exposure components	
CAPS (UFPM of diameter <0.18 μ m). The control, filtered air included a charcoal bed to remove VOCs	Ambient PM _{2.5} collected on Teflon filters in parallel with XAD resins below to collect VOCs
Physical and Chemical Analyses	
Particle count using condensation particle counter (Kleinman, Hamade et al. 2005), EC/OC monitored daily from glass fiber filters.	Prooxidant (DTT assay) and electrophile (GAPDH assay) content of Ambient PM (aqueous suspensions) and corresponding VOCs (DMSO solution)
Results of air component analyses	
On average, the VACES concentration factor was 12 (figure 2.1.5). VACES concentrates particles but loses semi VOCs which have been associated with pro-(Keebaugh, Sioutas et al. 2015) and anti-inflammatory responses (Iwamoto, Nishiyama et al. 2010).	High organic prooxidant content (35%) observed. The ambient Irvine prooxidant content was about 1/10 th that of Beijing and Mexico City so the 12 fold increase in concentration was an appropriate method to attain the higher levels of reactive species associated with the original report of ambient air based neurotoxicity from Mexico City.
Biological Protocols	
Animals exposed to CAPS for 5 hours per day, 4 days per week for 22 weeks. Protocol of (Kleinman, Hamade et al. 2005).	Cells exposed to DMSO solution of VOCs at concentrations of 3 m ³ /mL for 16 hours. Protocol of (Li, Venkatesan et al. 2000)
Biological analyses	
Animal responses to exposure: (see sections 2.2 and 2.3) 1. Behavior 2. Neurochemical: Dopamine, norepinephrine 3. Inflammatory cytokines: IL6, TNF α 4. Anti-inflammatory marker: HO-1 5. H α -synuclein concentration	Murine macrophage responses to VOCs: (Table 2.4.2) 1. Inflammatory cytokine: TNF α 2. Anti-inflammatory marker: HO-1
Biological Results	

<p>The chemical and biologic characterization of the CAPS (relatively low total mass per m³, organic and elemental carbon, prooxidant content of the particles) were likely explanatory factors for the minor extent of behavioral and brain deficits observed in our CAPS exposure - hα-Syn PD model. We had hypothesized that a longer exposure of 22 weeks may nonetheless have allowed for such deficits to develop. Although exposure to a more ‘toxic’ CAPS may have produced changes of greater magnitude, conclusions on their relevance to the human condition would remain uncertain. Assessing the effects of human AP exposure conditions in animal models may require the use of subtle behavioral tests that are reflective of changes in functional brain activity rather than changes in content of brain inflammatory markers or neurotransmitters.</p>	<p>Following stimulation by the vapor phase samples, HO-1 and TNFα expression by the macrophages had an inverse relationship, depending on the particle but not vapor parameter against which they were plotted. Thus, with particle prooxidant content as the X axis, HO-1 levels increased as TNFα levels decreased whereas particle organic carbon content as the X axis, the HO-1 levels decreased in TNFα levels increased. There was no correlation between the reactive components of the vapor phase with either protein.</p> <p>The correlation of the cell responses with particle, not vapor properties differs from prior studies.</p>
	<p>Comparison of Pearson correlation analyses between chemical and biological data (Table 5.5).</p>
	<p>Stimulation of HO-1 expression by SCAQMD vapor samples correlated with with vapor phase prooxidant content but had no effect on TNFα expression.</p>
<p>Toxicokinetics and exposure (see section 2.4.1)</p>	
<p>In vivo: continuous exposure with steady state levels dependent on rate of inhalation and rate of excretion.</p>	<p>In vitro: single exposure with time dependency on biotransformation.</p>
<p>Exposure comparison</p>	
<p>The steady state levels of reactive chemical species must be sufficient to overcome their removal by the biotransformation pathways available.</p>	<p>Typically, the concentrations used are high compared to concentration attained in vivo with ambient air in order to observe a significant response.</p>

In vivo summary	In vitro summary
	The in vitro studies provided a description of the exposure atmosphere in terms that could be used to relate the findings to those reported by others, most notably those from Mexico City where the neurologically relevant findings were made.
Although exposures in the three studies took place at sites with considerably higher pollutant content than those of this study, our study was considerably longer in duration. If the responsible agents for neurotoxicity are organic, exposure to low levels even for long periods could have minimal effect because of the ability of the host to eliminate the pollutants by biotransformation and excretion.	

Conclusions
<p>. We draw the following conclusions from the project as performed:</p> <ol style="list-style-type: none"> 1. The VACES approach to concentrating PM_{2.5} to approach the ambient concentrations in Mexico City was a reasonable one, as the device concentrated particles by a factor of 12, which, in turn increased the prooxidant content of the exposure atmosphere to levels close to those that we had found in our measurements (see Table 2.4.1). 2. The exposure performed in this study did not demonstrate significant neurotoxic events in spite of VACES concentration of ambient particles. 3. However, the ambient particles in Irvine differ quantitatively in terms of particle count and organic carbon content and qualitatively from other areas in the Los Angeles Basin in the nature of the cellular responses elicited. 4. The lower particle count and organic carbon could have resulted in a steady state exposure too low for a cumulative response. The results of figure 2.4.4 suggest that organic carbon content exceeding 25 µg/m³ would be necessary to obtain a pro-

inflammatory response in cells and the results of the other studies in table 2.5.2 suggest that to be the case.

3.0 References

- Amschl D, Neddens J, Havas D, Flunkert S, Rabl R, Romer H, Rockenstein E, Masliah E, Windisch M, Hutter-Paier B (2013) "Time course and progression of wild type alpha-synuclein accumulation in a transgenic mouse model." *BMC Neurosci* **14**:6.
- Araujo, J. A., B. Barajas, M. Kleinman, X. Wang, B. J. Bennett, K. W. Gong, M. Navab, J. Harkema, C. Sioutas, A. J. Lusis and A. E. Nel (2008). "Ambient particulate pollutants in the ultrafine range promote early atherosclerosis and systemic oxidative stress." *Circ Res* **102**(5): 589-596.
- Bayram, H., K. Ito, R. Issa, M. Ito, M. Sukkar and K. F. Chung (2006). "Regulation of human lung epithelial cell numbers by diesel exhaust particles." *Eur Respir J* **27**(4): 705-713.
- Calderon-Garciduenas, L., A. C. Solt, C. Henriquez-Roldan, R. Torres-Jardon, B. Nuse, L. Herritt, R. Villarreal-Calderon, N. Osnaya, I. Stone, R. Garcia, D. M. Brooks, A. Gonzalez-Maciuel, R. Reynoso-Robles, R. Delgado-Chavez and W. Reed (2008). "Long-term air pollution exposure is associated with neuroinflammation, an altered innate immune response, disruption of the blood-brain barrier, ultrafine particulate deposition, and accumulation of amyloid beta-42 and alpha-synuclein in children and young adults." *Toxicol Pathol* **36**(2): 289-310.
- Campbell, A., J. A. Araujo, H. Li, C. Sioutas and M. T. Kleinman (2008). "Particulate Matter Induced Enhancement of Inflammatory Markers in the Brains of Apolipoprotein E Knockout Mice." *Journal of nanoscience and nanotechnology* **8**(1-6).
- Carlsson, H., J. Aasa, N. Kotova, D. Vare, P. F. M. Sousa, P. Rydberg, L. Abramsson-Zetterberg and M. Tornqvist (2017). "Adductomic Screening of Hemoglobin Adducts and Monitoring of Micronuclei in School-Age Children." *Chem Res Toxicol* **30**(5): 1157-1167.
- Carlsson, H. and M. Tornqvist (2016). "An Adductomic Approach to Identify Electrophiles In Vivo." *Basic Clin Pharmacol Toxicol*.
- Carlsson, H., H. von Stedingk, U. Nilsson and M. Tornqvist (2014). "LC-MS/MS screening strategy for unknown adducts to N-terminal valine in hemoglobin applied to smokers and nonsmokers." *Chem Res Toxicol* **27**(12): 2062-2070.
- Cho, A., E. Di Stefano, Y. Ying, Rodriguez CE, D. Schmitz, Y. Kumagai, Miguel AH, Eiguren-Fernandez A, Kobayashi T, Avol E and F. JR (2004). "Determination of Four Quinones in Diesel Exhaust Particles, SRM 1649a and Atmospheric PM2.5." *Aerosol Science and Technology* **38**(S1): 68-81.
- Cho, A. K., C. Sioutas, A. H. Miguel, Y. Kumagai, D. A. Schmitz, M. Singh, A. Eiguren-Fernandez and J. R. Froines (2005). "Redox activity of airborne particulate matter at different sites in the Los Angeles Basin." *Environ Res* **99**(1): 40-47.
- Davies, G., E. A. Ghabbor and C. Steelink (2001). "Humic Acids: Marvelous Products of Soil Chemistry." *Journal of Chemical Education* **78**: 1609-1614.
- Deacon RM (2006) Assessing nest building in mice. *Nat Protoc* **1**:1117-1119.

- Delgado-Saborit, J. M., M. S. Alam, K. J. Godri Pollitt and R. M. Harrison (2013). "Analysis of atmospheric concentrations of quinones and polycyclic aromatic hydrocarbons in vapour and particulate phases. ." Atmospheric Environment **77**: 974-982.
- Di Stefano, E., A. Eiguren-Fernandez, R. J. Delfino, C. Sioutas, J. Froines and A. K. Cho (2009). "Determination of metal-based hydroxyl radical generating capacity of ambient and diesel exhaust particles." Inhalation Toxicology **21**(9): 731-738.
- Dinkova-Kostova, A. T., W. D. Holtzclaw, R. N. Cole, K. Itoh, N. Wakabayashi, Y. Katoh, M. Yamamoto and P. Talalay (2002). "Direct evidence that sulfhydryl groups of Keap1 are the sensors regulating induction of phase 2 enzymes that protect against carcinogens and oxidants." Proc Natl Acad Sci U S A **99**(18): 11908-11913.
- Dinkova-Kostova, A. T. and P. Talalay (2008). "Direct and indirect antioxidant properties of inducers of cytoprotective proteins." Mol Nutr Food Res **52** Suppl 1: S128-138.
- Eiguren-Fernandez, A. (2015). "Chemical reactivities of ambient air samples in three Southern California communities." J Air Waste Manag Assoc. **65**(3): 270-277.
- Ferrer-Sueta, G., B. Manta, H. Botti, R. Radi, M. Trujillo and A. Denicola (2011). "Factors affecting protein thiol reactivity and specificity in peroxide reduction." Chem Res Toxicol **24**(4): 434-450.
- Ghio, A., J. Stonehuerner, R. Pritchard, C. Piantadosi, D. Quigley, K. Dreher and D. Costa (1996). "Humic-like substances in air pollution particulates correlate with concentrations of transition metals and oxidant generation. ." Inhalation Toxicology **8**: 479-494.
- Gozzelino, R., V. Jeney and M. P. Soares (2009). "Mechanisms of cell protection by heme oxygenase-1." Annu Rev Pharmacol Toxicol **50**: 323-354.
- Iwamoto, N., A. Nishiyama, A. Eiguren-Fernandez, W. Hinds, Y. Kumagai, J. Froines, A. Cho and M. Shinyashiki (2010). "Biochemical and cellular effects of electrophiles present in ambient air samples." Atmospheric Environment **44**: 1483-1489.
- Iwamoto, N., D. Sumi, T. Ishii, K. Uchida, A. K. Cho, J. R. Froines and Y. Kumagai (2007). "Chemical knockdown of protein tyrosine phosphatase 1B by 1,2-naphthoquinone through covalent modification causes persistent transactivation of epidermal growth factor receptor." J Biol Chem **282**(46): 33396-33404.
- Jacobs, A. T. and L. J. Marnett (2010). "Systems analysis of protein modification and cellular responses induced by electrophile stress." Acc Chem Res **43**(5): 673-683.
- Jakober, C. A., M. J. Charles, M. J. Kleeman and P. G. Green (2006). "LC-MS analysis of carbonyl compounds and their occurrence in diesel emissions." Anal Chem **78**(14): 5086-5093.
- Jakober, C. A., S. G. Riddle, M. A. Robert, H. Destailats, M. J. Charles, P. G. Green and M. J. Kleeman (2007). "Ouinone emissions from gasoline and diesel motor vehicles." Environ Sci Technol **41**(13): 4548-4554.

- Kachur, A. V., K. D. Held, C. J. Koch and J. E. Biaglow (1997). "Mechanism of production of hydroxyl radicals in the copper-catalyzed oxidation of dithiothreitol." Radiat Res **147**(4): 409-415.
- Keebaugh, A. J., C. Sioutas, P. Pakbin, J. J. Schauer, L. B. Mendez and M. T. Kleinman (2015). "Is atherosclerotic disease associated with organic components of ambient fine particles?" Sci Total Environ **533**: 69-75.
- Kim, S., P. A. Jaques, M. Chang, T. Barone, C. Xiong, S. K. Friedlander and C. Sioutas (2001). "Versatile aerosol concentration enrichment system (VACES) for simultaneous in vivo and in vitro evaluation of toxic effects of ultrafine, fine and coarse ambient particles. Part II: Field evaluation." Journal of Aerosol Science **32**(11): 1299-1314.
- Kleinman, M. T., J. A. Araujo, A. Nel, C. Sioutas, A. Campbell, P. Q. Cong, H. Li and S. C. Bondy (2008). "Inhaled ultrafine particulate matter affects CNS inflammatory processes and may act via MAP kinase signaling pathways." Toxicol Lett **178**(2): 127-130.
- Kleinman, M. T., A. Hamade, D. Meacher, M. Oldham, C. Sioutas, B. Chakrabarti, D. Stram, J. R. Froines and A. K. Cho (2005). "Inhalation of Concentrated Ambient Particulate Matter near a Heavily Trafficked Road Stimulates Antigen-Induced Airway Responses in Mice." J. Air & Waste Manage. Assoc. **55**: 1277-1288.
- Kumagai, Y., S. Koide, K. Taguchi, A. Endo, Y. Nakai, T. Yoshikawa and N. Shimojo (2002). "Oxidation of proximal protein sulfhydryls by phenanthraquinone, a component of diesel exhaust particles." Chem Res Toxicol **15**(4): 483-489.
- Kumagai, Y., Y. Shinkai, T. Miura and A. K. Cho (2012). "The chemical biology of naphthoquinones and its environmental implications." Annu Rev Pharmacol Toxicol **52**: 221-247.
- Levesque, S., M. J. Surace, J. McDonald and M. L. Block (2011). "Air pollution & the brain: Subchronic diesel exhaust exposure causes neuroinflammation and elevates early markers of neurodegenerative disease." J Neuroinflammation **8**: 105.
- Li, N., P. Bhattacharya, G. Karavalakis, K. Williams, N. Gysel and N. Rivera-Rios (2014). "Emissions from commercial-grade charbroiling meat operations induce oxidative stress and inflammatory responses in human bronchial epithelial cells." Toxicol Rep **1**: 802-811.
- Li, N., S. Kim, M. Wang, J. Froines, C. Sioutas and A. Nel (2002). "Use of a stratified oxidative stress model to study the biological effects of ambient concentrated and diesel exhaust particulate matter." Inhal Toxicol **14**(5): 459-486.
- Li, N., C. Sioutas, A. Cho, D. Schmitz, C. Misra, J. Sempf, M. Wang, T. Oberley, J. Froines and A. Nel (2003). "Ultrafine particulate pollutants induce oxidative stress and mitochondrial damage." Environ Health Perspect **111**(4): 455-460.
- Li, N., M. I. Venkatesan, A. Miguel, R. Kaplan, C. Gujuluva, J. Alam and A. Nel (2000). "Induction of heme oxygenase-1 expression in macrophages by diesel exhaust particle chemicals and quinones via the antioxidant-responsive element." J Immunol **165**(6): 3393-3401.

- Li, N., M. Wang, T. D. Oberley, J. M. Sempf and A. E. Nel (2002). "Comparison of the pro-oxidative and proinflammatory effects of organic diesel exhaust particle chemicals in bronchial epithelial cells and macrophages." J Immunol **169**(8): 4531-4541.
- Lin, P. and J. Z. Yu (2011). "Generation of reactive oxygen species mediated by humic-like substances in atmospheric aerosols." Environ Sci Technol **45**(24): 10362-10368.
- LoPachin, R. M. and D. S. Barber (2006). "Synaptic cysteine sulfhydryl groups as targets of electrophilic neurotoxicants." Toxicol Sci **94**(2): 240-255.
- Masliah E, Rockenstein E, Veinbergs I, Mallory M, Hashimoto M, Takeda A, Sagara Y, Sisk A, Mucke L (2000) Dopaminergic loss and inclusion body formation in alpha-synuclein mice: implications for neurodegenerative disorders. Science **287**:1265-1269.
- Masliah E, Rockenstein E, Veinbergs I, Sagara Y, Mallory M, Hashimoto M, Mucke L (2001) beta-amyloid peptides enhance alpha-synuclein accumulation and neuronal deficits in a transgenic mouse model linking Alzheimer's disease and Parkinson's disease. Proc Natl Acad Sci U S A **98**:12245-12250.
- Mostofa, A. G., S. R. Punganuru, H. R. Madala, M. Al-Obaide and K. S. Srivenugopal (2017). "The Process and Regulatory Components of Inflammation in Brain Oncogenesis." Biomolecules **7**(2).
- Netto, L. E. and E. R. Stadtman (1996). "The iron-catalyzed oxidation of dithiothreitol is a biphasic process: hydrogen peroxide is involved in the initiation of a free radical chain of reactions." Arch Biochem Biophys **333**(1): 233-242.
- Park, H. S., S. R. Kim and Y. C. Lee (2009). "Impact of oxidative stress on lung diseases." Respirology **14**(1): 27-38.
- Poole, L. B. and K. J. Nelson (2008). "Discovering mechanisms of signaling-mediated cysteine oxidation." Curr Opin Chem Biol **12**(1): 18-24.
- Prester, T., Y. Zhang, S. R. Spencer, C. A. Wilczak and P. Talalay (1993). "The electrophile counterattack response: protection against neoplasia and toxicity." Adv Enzyme Regul **33**(12): 281-296.
- Rappaport, S. M., H. Li, H. Grigoryan, W. E. Funk and E. R. Williams (2012). "Adductomics: characterizing exposures to reactive electrophiles." Toxicol Lett **213**(1): 83-90.
- Ribeiro, D., M. Freitas, J. L. Lima and E. Fernandes (2015). "Proinflammatory Pathways: The Modulation by Flavonoids." Med Res Rev.
- Rockenstein E, Mallory M, Hashimoto M, Song D, Shults CW, Lang I, Masliah E (2002) "Differential neuropathological alterations in transgenic mice expressing alpha-synuclein from the platelet-derived growth factor and Thy-1 promoters". J Neurosci Res **68**:568-578.
- Rodriguez, C. E., J. M. Fukuto, K. Taguchi, J. Froines and A. K. Cho (2005). "The interactions of 9,10-phenanthrenequinone with glyceraldehyde-3-phosphate dehydrogenase (GAPDH), a potential site for toxic actions." Chem Biol Interact **155**: 97-110.

- Samet, J. M., R. Silbajoris, W. Wu and L. M. Graves (1999). "Tyrosine phosphatases as targets in metal-induced signaling in human airway epithelial cells." Am J Respir Cell Mol Biol **21**(3): 357-364.
- Samet, J. M. and T. L. Tal (2010). "Toxicological disruption of signaling homeostasis: tyrosine phosphatases as targets." Annu Rev Pharmacol Toxicol **50**: 215-235.
- Shinkai, Y., D. Sumi, I. Fukami, T. Ishii and Y. Kumagai (2006). "Sulforaphane, an activator of Nrf2, suppresses cellular accumulation of arsenic and its cytotoxicity in primary mouse hepatocytes." FEBS Lett **580**(7): 1771-1774.
- Shinyashiki, M., A. Eiguren-Fernandez, D. A. Schmitz, E. Di Stefano, N. Li, W. P. Linak, S. H. Cho, J. R. Froines and A. K. Cho (2009). "Electrophilic and redox properties of diesel exhaust particles." Environ Res **109**: 239-244.
- Shinyashiki, M., C. E. Rodriguez, E. W. Di Stefano, C. Sioutas, R. J. Delfino, Y. Kumagai, J. R. Froines and A. K. Cho (2008). "On the interaction between glyceraldehyde-3-phosphate dehydrogenase and airborne particles: Evidence for electrophilic species. ." Atmospheric Environment **42**: 517-529.
- Sun, G., K. Crissman, J. Norwood, J. Richards, R. Slade and G. E. Hatch (2001). "Oxidative interactions of synthetic lung epithelial lining fluid with metal-containing particulate matter." Am J Physiol Lung Cell Mol Physiol **281**(4): L807-815.
- Taguchi, K., M. Shimada, S. Fujii, D. Sumi, X. Pan, S. Yamano, T. Nishiyama, A. Hiratsuka, M. Yamamoto, A. K. Cho, J. R. Froines and Y. Kumagai (2008). "Redox cycling of 9,10-phenanthraquinone to cause oxidative stress is terminated through its monoglucuronide conjugation in human pulmonary epithelial A549 cells." Free Radic Biol Med **44**(8): 1645-1655.
- Totlandsdal, A. I., J. Ovreivik, R. E. Cochran, J. I. Herseth, A. K. Bolling, M. Lag, P. Schwarze, E. Lilleaas, J. A. Holme and A. Kubatova (2014). "The occurrence of polycyclic aromatic hydrocarbons and their derivatives and the proinflammatory potential of fractionated extracts of diesel exhaust and wood smoke particles." J Environ Sci Health A Tox Hazard Subst Environ Eng **49**(4): 383-396.
- Valavanidis, A., K. Fiotakis, T. Vlahogianni, V. Papadimitriou and V. Pantikaki (2006). "Determination of Selective Quinones and Quinoid Radicals in Airborne Particulate Matter and Vehicular Exhaust Particles. " Environmental Chemistry **3**(2): 118-123.
- Valko, M., H. Morris and M. T. D. Cronin (2005). "Metals, Toxicity and Oxidative Stress." Current Medicinal Chemistry **12**: 1161-1208
- Verma, V., T. Fang, L. Xu, R. E. Peltier, A. G. Russell, N. L. Ng and R. J. Weber (2015). "Organic aerosols associated with the generation of reactive oxygen species (ROS) by water-soluble PM_{2.5}." Environ Sci Technol **49**(7): 4646-4656.
- Verma, V., P. Pakbin, K. L. Cheung, A. K. Cho, J. J. Schauer, M. M. Shafer, M. T. Kleinman and C. Sioutas (2011). "Physicochemical and oxidative characteristics of semi-volatile

components of quasi-ultrafine particles in an urban atmosphere." Atmospheric Environment **45** (2011) **45**: 1025-1033.

Verma, V., Y. Wang, R. El-Afifi, T. Fang, J. Rowland, A. G. Russel and R. J. Weber (2015).

"Fractionating Ambient Humic-like Substances (HULIS) for their reactive oxygen species activity - Assessing the importance of quinones and atmospheric aging." Atmospheric Environment, **in press**.

Wu, W., P. A. Bromberg and J. M. Samet (2013). "Zinc ions as effectors of environmental oxidative lung injury." Free Radic Biol Med **65**: 57-69.

Yang, B., P. Ma, J. Shu, P. Zhang, J. Huang and H. Zhang (2018). "Formation mechanism of secondary organic aerosol from ozonolysis of gasoline vehicle exhaust." Environ Pollut **234**: 960-968.

Zheng, G., K. He, F. Duan, Y. Cheng and Y. Ma (2013). "Measurement of humic-like substances in aerosols: a review." Environ Pollut **181**: 301-314.

Appendix 1: Abbreviations

Air: ambient air

AP: air pollution

AQ: 9,10-anthroquinone

BCA Assay Kit: bicinchoninic acid assay kit

1,4- BQ: 1,4-benzoquinone

CAPS: concentrated particles

CARB: California Air Resources Board

DA: dopamine

DEP: diesel exhaust particles

DHBA: dihydroxybenzoic acid

dob: date of birth

DTT: dithiothreitol

EC: elemental carbon

ELISA: enzyme-linked immunosorbent assay

Exp-st: exposure-start

FA: filtered air

FeSO₄: ferrous sulfate

GAPDH: glyceraldehyde-3-phosphate dehydrogenase

HEPA: high efficiency particulate air

HO-1: heme oxygenase-1

HPLC: high-performance liquid chromatography

HULIS: humic-like substances

h α -Syn: human alpha-synuclein

H₂O₂: hydrogen peroxide

IL1: interleukin 1

IL6: interleukin 6

J-DEP: Japanese-diesel exhaust particle sample

LPS: lipopolysaccharide

KEAP 1: kelch-like ECH-associated protein 1

MALDI TOF/MS: matrix-assisted laser desorption ionization time-of-flight mass spectrometry

MAP kinase: mitogen-activated protein kinase

M-PER: mammalian protein extraction reagent

NADPH: nicotinamide adenine dinucleotide phosphate

NQ 2- : 2- naphthoquinone

NQ 1,4- : 1,4-naphthoquinone

NE: norepinephrine

NEM: N-ethyl maleimide

NF- κ B: nuclear factor-kappaB

Nrf-2: nuclear factor erythroid 2-related factor 2

O₂⁻ : superoxide

OC: organic carbon

OH• : hydroxyl radical

PAH: polynuclear aromatic hydrocarbon

PD: Parkinson's Disease

PM_{2.5}: fine particles with a diameter of 2.5 μ m or less

PQ: 9,10-phenanthroquinone

PTP1B: Protein tyrosine phosphatase 1B

9,10-PQ: 9,10-phenanthroquinone

PRR: pattern recognition receptors

RAM estimates: Estimates of particle number from a DataRAM Model DK-2000(MIE) with sampling at 1.7 L/min.

ROS: reactive oxygen species

SB: San Bernardino

SCAQMD: South Coast Air Quality Management District (Railyard study)

TNF α : tumor necrosis factor alpha

t-turn: time to orient downward

t-turn: total time to descend

UCI: University of California, Irvine

UCLA: University of California, Los Angeles

UFPM: ultrafine particulate matter

VACES: versatile aerosol concentration enrichment system

VOC: volatile organic compounds

Appendix 2: Animal cohorts and calendar

Cohort#	1	2	3	4			
dob (ave)	5-Mar	15-Mar	12-Apr	28-Apr			
Transfer	23-Jun						
		Transfer	30-Jun				
Behav	30-Jun						
		Behav	7-Jul				
(age 17 wks) (T - F)			Transfer	21-Jul			
Exp-st Wk 1	7-Jul	(age 16 wks) (T - F)					
2	14-Jul	Exp-st Wk 1	14-Jul	Behav	27-Jul		
3	21-Jul	2	21-Jul		Transfer	11-Aug	
4	28-Jul	3	28-Jul	(age 16 wks) (T - F)			
5	4-Aug	4	4-Aug	Exp-st Wk 1	4-Aug	Behav	17-Aug
6	11-Aug	5	11-Aug	2	11-Aug		
7	18-Aug	6	18-Aug	3	18-Aug	(age 16 wks) (T - F)	
8	25-Aug	7	25-Aug	4	25-Aug	Exp-st Wk 1	25-Aug
9	1-Sep	8	1-Sep	5	1-Sep	2	1-Sep
10	8-Sep	9	8-Sep	6	8-Sep	3	8-Sep
11	15-Sep	10	15-Sep	7	15-Sep	4	15-Sep
12	22-Sep	11	22-Sep	8	22-Sep	5	22-Sep
13	29-Sep	12	29-Sep	9	29-Sep	6	29-Sep
14	6-Oct	13	6-Oct	10	6-Oct	7	6-Oct
15	13-Oct	14	13-Oct	11	13-Oct	8	13-Oct
16	20-Oct	15	20-Oct	12	20-Oct	9	20-Oct
17	27-Oct	16	27-Oct	13	27-Oct	10	27-Oct
18	3-Nov	17	3-Nov	14	3-Nov	11	3-Nov
19	10-Nov	18	10-Nov	15	10-Nov	12	10-Nov
20	17-Nov	19	17-Nov	16	17-Nov	13	17-Nov
21	22-Nov	20	22-Nov	17	22-Nov	14	*11/22/2015
22	30-Nov	21	30-Nov	18	30-Nov	15	30-Nov
Behavior	7-Dec	22	7-Dec	19	7-Dec	16	*12/7/2015
Sacrifice	10-Dec	Behavior	14-Dec	20	14-Dec	17	14-Dec
		Sacrifice	17-Dec	21	21-Dec	18	21-Dec
wt	10 mice			22	28-Dec	19	28-Dec
Syn+	10 mice	wt	10 mice	Behavior	4-Jan	20	4-Jan
		Syn+	5 mice	Sacrifice	7-Jan	21	11-Jan
						22	18-Jan
AP Exposures				wt	16 mice	Behavior	25-Jan
5 hours/day 4 days/week				Syn+	16 mice	Sacrifice	28-Jan
Tues-Fri	white boxes					wt	8 mice
*Sun-Wed						Syn+	13 mice
*Mon-Thurs							

Appendix 2 - Legend for Animal cohorts and calendar

Organization of the four cohorts were based on mouse availability in terms of age and the breeding of male transgenic heterozygotes. Each of the four cohorts contained wildtype and h α Syn mice that were randomly divided into either the air or AP condition. Microchips were implanted in the mice to facilitate and verify daily and weekly placement into their designated exposure condition. The availability of mice that could enter the study at approximately 4 months of age determined the final numbers for each condition. There was a 1 week acclimation period (Transfer: from the Blurton-Jones Colony to the Kleinman housing facility) to allow the mice to adjust to their new environment. Then, there was a 1 week behavioral testing period to obtain baseline measure of the behavioral tests. The mice were then exposed to 22 weeks of continuous exposure, Tues through Friday, of either air or AP. The exceptions to the Tues-Fri protocol are highlighted in 'orange' or 'light green'; these modifications were due to staff absences during Thanksgiving, Christmas and New Year's holidays. After the 22 weeks of exposure, the behavioral tests were again administered, followed by animal sacrifice and brain dissection.

This Table shows that each of the 4 cohorts contained adequate numbers of mice for distribution across all four conditions. Although, there was some staggering of the cohorts, there nonetheless was significant overlap in the exposure time period, indicating that the mice were essentially exposed to the same AP content for most of the 22 weeks.

Appendix 3: Selection and characteristics of the animal model

Housing and experimental use of the animals were performed in strict accordance with the National Institutes of Health guidelines. All animal experiments were approved by the UCLA Institutional Animal Care and Use Committee, known as the Chancellor's Animal Research Committee (ARC), ARC # 2014-134-01 "Behavioral and CNS Pathology Associated with Ultrafine Particle Exposure in an a-Syn Transgenic Mouse Model of Parkinson' Disease" (Approval Period from 12/11/2014 through 12/10/2017). Animals were housed under barrier conditions in a vented isolation caging system (Animal Care Systems, Littleton, CO) where they were provided with PROLAB RMH 2400 lab chow (PMI Nutrition International Inc., Brentwood, MO) and water ad libitum. Mice were maintained on a 12-h light/12-h dark cycle.

Accumulation and toxic conversion of protofibrils of α -Syn has been associated with neurological disorders such as PD, Lewy body disease, multiple system atrophy and Alzheimer's disease. In recent years, modeling these disorders in transgenic mice has helped improve understanding of the pathogenesis of these diseases In particular, overexpression of α -Syn in transgenic mice in a region- and cell-specific manner has been shown to result in degeneration of selective circuitries accompanied by motor deficits and inclusion formation similar to what is

found in PD and related disorders. Accordingly, most transgenic models have been focused on investigating the *in vivo* effects of α -Syn accumulation using neuronal specific promoters

Among these models, overexpression of h α -Syn under the regulatory control of the platelet-derived growth factor β (PDGF β) promoter has been shown to result in motor deficits, dopaminergic loss, and formation of inclusion bodies (Masliah et al., 2000). These mice replicate features of human synucleinopathies such as abnormal accumulation of h α -Syn, increased phosphorylation of h α -Syn and high levels of ubiquitin, in cortical and subcortical regions of the brain. Specifically, transgenic h α -Syn mRNA is expressed at high levels in the hippocampus, neocortex, olfactory bulb and the substantia nigra, whereas expression is largely absent from other parts of the brain (Rockenstein et al., 2002). Strong immunoreactivity of human α -Syn protein is evident in different subsets of neuronal somata in the above-mentioned areas, and both expression and aggregation of h α -Syn increase as the animals age. This is particularly evident for the h α -Syn levels in the hippocampus and striatum regions that are present during the age/time period of the study, ~ 4 to 9 months. Further, this strain of mice was shown to develop motor and cognitive deficits, and exhibit Lewy body-like inclusions between 6 and 12 months of age, together with other deficits associated with PD (Amschl et al., 2013). This distinct histopathological pattern favored testing for potential differences in regional sensitivity (hippocampus, striatum) to negative effects of AP exposure as evidenced by neurochemical deficits, increases of human α -Syn accumulation, and expression of neuroinflammatory and oxidative stress markers.

We were fortunate to have the opportunity to collaborate with our colleague at UCI (Professor Mathew Blurton-Jones of the School of Biological Sciences) who was maintaining a colony of both C57BL/6J wild type mice and transgenic mice with the PDGF β promoter of α -Syn. His willingness to collaborate on this project with us was critically important to our study design since his mouse facility could deliver the required large number of age-matched transgenic males (with verification by PCR) to Dr. Kleinman's research and mouse facility located nearby on the same campus. Mice were bred in-house on a C57B6/J background (wild type littermates serves as the control groups). All experiments were performed with hemizygous D-Line male mice and corresponding non-transgenic littermates. Each cohort entered into the study at ~ 4 months of age. Each cohort contained animals representing all four conditions: h α -Syn mice and wild-type mice either exposed to CAPS or filtered air. The exposure continued for 22 weeks (5h/d for 4d/week), consecutively. Subsequently, the mice were tested for behavioral alterations at 4d following the last day of the last week of exposure and then sacrificed 3d later, i.e., one week after their last AP exposure.

Appendix 4: Statistical analysis parameters for the h⁺-Syn mice studies

Statistical analyses was performed using *GraphPad Prism 7* software (*GraphPad* software, Inc, La Jolla, CA). Statistics parameters are shown for selected wildtype and h⁺-Syn datasets

Figure 2.2.1 Pole Test**Unpaired Student's t test: total (rotate and descent); final (post-exposure)****Unpaired Student's test: rotate; final (post exposure)**

	Data Set-A		Data Set-A
Table Analyzed	Syn: total final	Table Analyzed	Syn: rotate final
Column A	syn air	Column A	syn air
vs	vs	vs	vs
Column B	syn exp	Column B	syn exp
Unpaired t test		Unpaired t test	
P value	0.6454	P value	0.9641
P value summary	ns	P value summary	ns
Are means signif. different? (P < 0.05)	No	Are means signif. different? (P < 0.05)	No
One- or two-tailed P value?	Two-tailed	One- or two-tailed P value?	Two-tailed
t, df	t=0.4640 df=36	t, df	t=0.04537 df=36
How big is the difference?		How big is the difference?	
Mean ± SEM of column A	9.982 ± 1.318 N=15	Mean ± SEM of column A	4.408 ± 0.9842 N=15
Mean ± SEM of column B	10.66 ± 0.8013 N=23	Mean ± SEM of column B	4.456 ± 0.5573 N=23
Difference between means	-0.6741 ± 1.453	Difference between means	-0.04765 ±
95% confidence interval	-3.622 to 2.274	95% confidence interval	1.050
R squared	0.005946	R squared	-2.179 to 2.084
F test to compare variances		F test to compare variances	0.00005717
F,DFn, Dfd	1.764, 14, 22	F,DFn, Dfd	
P value	0.2260	P value	
P value summary	ns	P value summary	2.034, 14, 22
Are variances significantly different?	No	Are variances significantly different?	0.1316
			ns

**Figure 2.2.2. Challenging Beam Test –
back limb
final – initial**

Paired Student’s test: Syn-exp

	Data Set-A
Table Analyzed	Syn-exp
Column A	Back initial
vs	vs
Column B	Back final
Paired t test	
P value	0.0345
P value summary	*
Are means signif. different? (P < 0.05)	Yes
One- or two-tailed P value?	Two-tailed
t, df	t=2.298 df=17
Number of pairs	18
How big is the difference?	-0.06233
Mean of differences	-0.1196 to -
95% confidence interval	0.005111
R squared	0.2371
How effective was the pairing?	
Correlation coefficient (r)	0.1600
P Value (one tailed)	0.2629
P value summary	ns
Was the pairing significantly effective?	No

Paired Student’s test: Syn-air

	Data Set-A
Table Analyzed	Syn-air
Column A	Back initial
vs	vs
Column B	Back final
Paired t test	
P value	0.8422
P value summary	ns
Are means signif. different? (P < 0.05)	No
One- or two-tailed P value?	Two-tailed
t, df	t=0.2028 df=14
Number of pairs	15
How big is the difference?	-0.006467
Mean of differences	-0.07486 to
95% confidence interval	0.06193
R squared	0.002930
How effective was the pairing?	
Correlation coefficient (r)	0.08511
P Value (one tailed)	0.3815
P value summary	ns
Was the pairing significantly effective?	No

**Figure 2.2.2 Challenging Beam Test –
back limb
final - initial**

Paired Student’s test: wt-exp

	Data Set-A
Table Analyzed	wt-exp
Column A	Back initial
vs	vs
Column B	Back final
Paired t test	
P value	0.0381
P value summary	*
Are means signif. different? (P < 0.05)	Yes
One- or two-tailed P value?	Two-tailed
t, df	t=2.207 df=22
Number of pairs	23
How big is the difference?	-0.05283
Mean of differences	-0.1025 to -
95% confidence interval	0.003183
R squared	0.1813
How effective was the pairing?	
Correlation coefficient (r)	0.1769
P Value (one tailed)	0.2096
P value summary	ns
Was the pairing significantly effective?	No

Paired Student’s test: wt-air

	Data Set-A
Table Analyzed	wt-air
Column A	Back initial
vs	vs
Column B	Back final
Paired t test	
P value	0.4717
P value summary	ns
Are means signif. different? (P < 0.05)	No
One- or two-tailed P value?	Two-tailed
t, df	t=0.7304 df=26
Number of pairs	27
How big is the difference?	0.0140
Mean of differences	-0.02541 to
95% confidence interval	0.05341
R squared	0.02011
How effective was the pairing?	
Correlation coefficient (r)	0.5171
P Value (one tailed)	0.0029
P value summary	**
Was the pairing significantly effective?	Yes

Figure 2.2.3 Nestlet/Nest building

Mann-Whitney test

Syn/exp vs Syn/air 2h

Syn/exp vs Syn/air 18h

	Data Set-A		Data Set-A
Table Analyzed	Data 1	Table Analyzed	air Syn 18h
Column A	air-Syn 2h	Column A	air-Syn 18h
vs	vs	vs	vs
Column B	exp-Syn 2h	Column B	exp-Syn 18h
Mann Whitney test		Mann Whitney test	
P value	0.7694	P value	0.1136
Exact or approximate P value?	Gaussian	Exact or approximate P value?	Gaussian
P value summary	Approximation	P value summary	Approximation
Are medians signif. different? (P < 0.05)	ns	Are medians signif. different? (P < 0.05)	ns
One- or two-tailed P value?	No	One- or two-tailed P value?	No
Sum of ranks in column A,B	Two-tailed	Sum of ranks in column A,B	Two-tailed
Mann-Whitney U	313 , 390	Mann-Whitney U	274.5 , 428.5
	160.0		121.5

Figure 2.2.4 Y maze spontaneous alternations

Unpaired Student's t test:

air-syn vs exp-syn

Total arm visits

	Data Set-A
Table Analyzed	Data 1
Column A	air-Syn
vs	vs
Column B	exp-Syn
Unpaired t test	
P value	0.3218
P value summary	ns
Are means signif. different? (P < 0.05)	No
One- or two-tailed P value?	Two-tailed
t, df	t=1.005 df=35
How big is the difference?	19.12 ± 1.209
Mean ± SEM of column A	N=17
Mean ± SEM of column B	17.00 ± 1.646
Difference between means	N=20
95% confidence interval	2.118 ± 2.107
R squared	-2.163 to 6.398
	0.02805
F test to compare variances	
F,DFn, Dfd	
P value	2.181, 19, 16
P value summary	0.1207
Are variances significantly different?	ns
	No

Alternations (fraction: consecutive/3 arm visits / total visits)

	Data Set-A
Table Analyzed	Alternations
Column A	air-Syn
vs	vs
Column B	exp-Syn
Unpaired t test	
P value	0.6848
P value summary	ns
Are means signif. different? (P < 0.05)	No
One- or two-tailed P value?	Two-tailed
t, df	t=0.4094 df=35
How big is the difference?	0.6718 ± 0.02916
Mean ± SEM of column A	N=17
Mean ± SEM of column B	0.6465 ± 0.05114
Difference between means	N=20
95% confidence interval	0.02526 ± 0.06172
R squared	-0.1001 to 0.1506
	0.004765
F test to compare variances	
F,DFn, Dfd	
P value	3.619, 19, 16
P value summary	0.0123
Are variances significantly different?	*
	Yes

Data 1

Figure 2.3.4 Striatum dopamine (DA) content.**Unpaired Student's t test:**

air-syn vs exp-syn The DA exp-syn content was decreased by ~ 10% relative to that for DA air-syn, but it was not significantly different.

Table Analyzed	Data 1
Column C	air-syn
vs	vs
Column D	exp-syn

Unpaired t test	
P value	0.2583
P value summary	ns
Are means signif. different? (P < 0.05)	No
One- or two-tailed P value?	Two-tailed
t, df	t=1.153 df=29

How big is the difference?	
Mean \pm SEM of column C	6.928 \pm 0.3635 N=16
Mean \pm SEM of column D	6.376 \pm 0.3066 N=15
Difference between means	0.5520 \pm 0.4787
95% confidence interval	-0.4270 to 1.531
R squared	0.04384

F test to compare variances	
F,DFn, Dfd	1.500, 15, 14
P value	0.4547
P value summary	ns
Are variances significantly different?	No